Mineralium Deposita (2019) 54:329–346
https://doi.org/10.1007/s00126-018-0809-1

ARTICLE

^{40}Ar-^{39}Ar dating of Archean iron oxide Cu-Au and Paleoproterozoic granite-related Cu-Au deposits in the Carajás Mineral Province, Brazil: implications for genetic models

Peter J. Pollard[1] · Roger G. Taylor[2] · Lisa Peters[3] · Fernando Matos[4] · Cantidiano Freitas[4] · Lineu Saboia[4] · Sergio Huhn[4]

Received: 9 July 2017 / Accepted: 13 April 2018 / Published online: 2 May 2018

Abstract

^{40}Ar-^{39}Ar dating of biotite from IOCG and granite-related Cu-Au deposits in the Carajás Mineral Province provides evidence for the timing of mineralization and constraints on genetic models of ore formation. Ages of biotite from greisen and quartz-rich vein and breccia deposits, Alvo 118—1885 ± 4 Ma, Breves—1886 ± 5 Ma, Estrela—1896 ± 7 Ma, and Gameleira—1908 ± 7 Ma, demonstrate the close temporal relationship between Cu-Au mineralization and subjacent A-type granites. Mineralization is hosted within granite cupolas (Breves) or in vein/breccia systems emanating from the cupolas (Estrela and Gameleira), consistent with a genetic relationship of mineralization to the B-Li-F-rich granites. Plateau and minimum ages of biotite from IOCG deposits, including Igarapé Bahia, Cristalino, Corta Goela, and GT34, range from 2537 ± 6 Ma to 2193 ± 4 Ma. The ^{40}Ar-^{39}Ar age of biotite from Igarapé Bahia (2537 ± 6 Ma) is similar to a previous SHRIMP ^{207}Pb-^{206}Pb age for monazite of 2575 ± 12 Ma when the uncertainties in the respective analyses and standards are taken into account. The age spectrum for biotite from Cristalino shows increasing ages for successive steps, consistent with post-crystallization Ar loss, and the age of 2388 ± 5 Ma for the last three steps is considered a minimum age for Cu-Au mineralization. The age of biotite from the GT34 prospect (2512 ± 7 Ma) coincides with a previously identified period of basement reactivation and may indicate the formation of Cu-Au mineralization at this time or resetting of biotite from an older mineralization event at this time. At Corta Goela, within the Canaã Shear Zone, the biotite age of 2193 ± 4 Ma lies between the ages of IOCG (2.57–2.76 Ga) and granite-related Cu-Au (~ 1.88 Ga) deposits elsewhere in the Carajás district but is similar to previously reported ^{40}Ar-^{39}Ar ages for amphibole from Sossego, possibly indicating that mineralization at both Sossego and Corta Goela was affected by a thermal event at this time. The Paleoproterozoic Cu-Au deposits are commonly hosted within Neoarchean IOCG alteration systems and the common occurrence of potassic alteration (especially biotite) in both types of deposits means that special care is required in interpreting the paragenesis of alteration in both types of deposits. The Paleoproterozoic Cu-Au deposits are reduced, and sulfur- and quartz-rich deposits lacking in major amounts of iron oxides and are therefore unlike IOCG deposits. Instead, they share many characteristics in common with widespread Paleoproterozoic Sn-W deposits in the Amazon Craton, including close spatial and temporal relationships with reduced A-type B-Li-F granites, and the occurrence of greisen and quartz-rich vein/breccia systems within and above granite cupolas. The occurrence of sericitic alteration in the Paleoproterozoic Cu-Au deposits is not evidence for an upward transition to sericitic alteration in IOCG deposits in the Carajás Mineral Province.

Editorial handling: S. Hagemann

Electronic supplementary material The online version of this article (https://doi.org/10.1007/s00126-018-0809-1) contains supplementary material, which is available to authorized users.

✉ Peter J. Pollard
Peter@PeterPollard.com

[1] Pollard Geological Services Pty. Ltd., 7 Jillinda Place, The Gap, Queensland 4061, Australia

[2] 15 Burns Street, Invermay, TAS 7248, Australia

[3] New Mexico Bureau of Geology and Mineral Resources, 801 Leroy Place, Socorro, NM 87801, USA

[4] Vale S.A., Centro de Desenvolvimento Mineral, BR 381, km 450, Dist. Industrial Simão da Cunha, Santa Luzia, MG 33.040-900, Brazil

Introduction

The Carajás Mineral Province is located at the southeastern margin of the Amazon Craton, Brazil. Since discovery of the Carajás iron deposits in 1967 (Tolbert et al. 1971) and the Salobo copper-gold deposit in 1977 (Lindenmayer and Teixeira 1999), Carajás has emerged as a world-class iron and copper-gold province. In addition, the province hosts major manganese (Azul), nickel (Vermelho, Luanga), and gold-PGE (Serra Pelada) deposits (Fig. 1).

The Cu-Au deposits include large (> 200 Mt) iron oxide copper-gold deposits (e.g., Cristalino, Igarapé Bahia, Salobo, and Sequeirinho; Fig. 1) as well as a group of smaller (mostly < 50 Mt) granite-related Cu-Au (W-Sn-Bi) deposits, including Águas Claras, Breves, Estrela, and Gameleira (Grainger et al. 2008). Copper-gold deposits are hosted mainly in volcano-sedimentary rocks of the Itacaiúnas Supergroup as well as in basement rocks of the Xingu gneiss complex and Rio Maria granitoid-greenstone terrain (Fig. 1).

Dating of Cu-Au deposits in the Carajás Mineral Province indicates three main episodes of mineralization at ca. 2.7 Ga (e.g., Sequeirinho, Moreto et al. 2015a), 2.57 Ga (e.g., Salobo, Requia et al. 2003 and Igarapé Bahia, Tallarico et al. 2005), and ca.1.88 Ga (e.g., Breves, Tallarico et al. 2004). Gameleira has an Archean Re-Os molybdenite age (2614 ± 14 Ma, Marschik et al. 2005) and Lindenmayer et al. (2005) refer to an unpublished Archean Re-Os molybdenite age for Estrela.

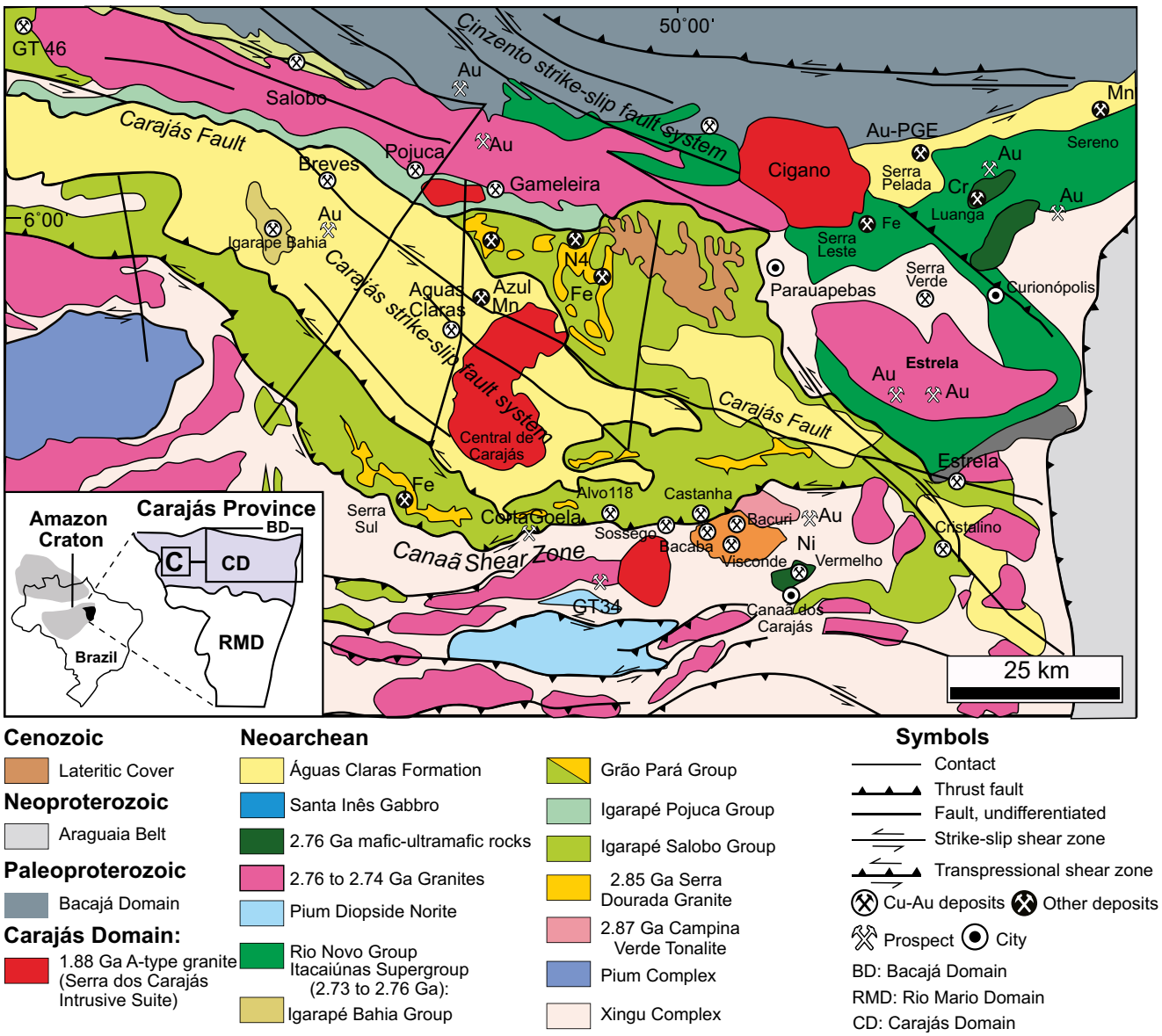

Fig. 1 Geological map of the Carajás Domain. **a** Location in Brazil. **b** Location of the Carajás Domain in the Carajás Province. **c** Geological map of the Carajás Domain (Vasquez et al. 2008)

Both deposits have strong geological and mineralogical affinities with the Paleoproterozoic deposits.

We report ^{40}Ar-^{39}Ar ages for biotite from eight copper-gold deposits and prospects in the Carajás district. These results, together with other geochronological data, help to constrain the ages of the copper-gold mineralization and models for the formation of the deposits. This raises questions concerning the classification of the Paleoproterozoic Cu-Au deposits as members of the iron oxide-copper-gold (IOCG) clan and suggests the likelihood that they instead form part of a granite-related group of Cu-Au deposits that are essentially greisen and quartz-rich vein/breccia systems linked to Paleoproterozic B-Li-F-Sn granites which are widespread in the Amazon Craton.

Regional geology

The Carajás Province includes basement gneiss and migmatite of the Xingu Complex, granulite of the Pium Complex, and the Bacaba tonalite with ages ~ 3.0 Ga (Pidgeon et al. 2000; Moreto et al. 2011) and to the south, the Rio Maria Domain composed of greenstone belts, granite, and mafic-ultramafic rocks. These basement rocks are overlain by a 2.76–2.73 Ga (Machado et al. 1991; Tallarico et al. 2005) sequence of metavolcanic and metasedimentary rocks and banded iron formations of the Rio Novo Group and Itacaiúnas Supergroup, and ~ 2.68 Ga (Trendall et al. 1998) sandstone and siltstone of the Águas Claras Formation. The major units of the Itacaiúnas Supergroup comprise the Salobo, Igarapé Pojuca, Grão Pará, and Igarapé Bahia groups (e.g., Docegeo 1988). These sequences were deposited in a basin formed in an intracontinental or continental arc setting (Dardenne et al. 1988; Machado et al. 1991) and have been deformed by major NW-trending transcurrent fault systems including the Cinzento and Carajás strike slip systems and the Carajás fault. These were reactivated as transtensional and transpressional systems in the Late Archean and as transpressional and extensional systems in the Proterozoic (Pinheiro and Holdsworth 1997; Holdsworth and Pinheiro 2000). The metamorphic grade ranges from greenschist facies in the southern part of the Carajás domain to amphibolite facies in the Salobo Group in the northern part of the domain (Machado et al. 1991; Olszewski et al. 1989).

Four main episodes of granite intrusion can be recognized within the Carajás Province: Mesoarchean (~ 3.0 Ga Sequeirinho Granite and Bacaba Tonalite, Moreto et al. 2011, 2015a; 2.87–2.83 Ga Campina Verde tonalite complex and Cruzadão granite, Feio, 2013), Neoarchean A-type granitoids (~ 2.75–2.70 Ga Estrela, Planalto, Serro de Rabo, Sossego and Curral granites, Barros et al. 2009; Feio et al., 2012; Huhn et al. 1999a; Sardinha et al. 2006), ~ 2.57 Ga Old Salobo and Itacaiúnas Granites (Machado et al. 1991; Souza et al. 1996), and Paleoproterozoic (~ 1.88 Ga) A-type granites (e.g., Carajás and Cigano granites (Machado et al. 1991)). The Luanga mafic-ultramafic complex was emplaced at ~ 2.75 Ga (Machado et al. 1991).

Iron-oxide Cu-Au deposits

The main iron-oxide copper-gold deposits in the Carajás Mineral Province include Salobo, Cristalino, Sequeirinho (part of the Sossego-Curral-Sequeirinho group of deposits referred to collectively as Sossego), and Igarapé Bahia (Table 1) as well as a number of other deposits/prospects including Alvo GT46 (Silva et al. 2005), Bacuri (Melo et al. 2014), Bacaba (Augusto et al. 2008), Visconde (Silva et al. 2015), and Castanha Jatobá and Pedra Branca (Moreto et al. 2015b). Most deposits have widespread early sodic and/or sodic-calcic alteration but this is weakly developed or absent at Igarapé Bahia. The deposits have major stages of K and Fe metasomatism represented by various combinations of K-feldspar, biotite, fayalite, grunerite, actinolite, magnetite, and chlorite (Table 1). This is typically overprinted by breccia-, vein-, and replacement-style Cu-Au mineralization that includes combinations of chalcopyrite, bornite, chalcocite, cobaltite, molybdenite, gold, and a variety of minor phases that are commonly accompanied by fluorite, apatite, and tourmaline (Table 1). The deposits have sulfur-poor sulfide assemblages and generally quartz-poor mineralization, with enrichment in LREE and variable enrichment in Co, Ni, Pb, and Zn (Grainger et al. 2008). Minor Sn as cassiterite occurs at Igarapé Bahia and Sequeirinho while Igarapé Bahia contains minor tungsten in the form of ferberite and scheelite (Table 1).

The IOCG deposits appear to be contemporaneous with high-K calc-alkaline to shoshonitic intrusions which were emplaced during ductile deformation. The ages of mineralization at Salobo (Re-Os molybdenite age 2576 ± 8 Ma, Requia et al. 2003) and Igarapé Bahia (^{207}Pb-^{206}Pb monazite age 2575 ± 12, Tallarico et al. 2005) are similar to the 2.57 Ga U-Pb zircon ages of the Itacaiúnas and Old Salobo granites (Machado et al. 1991; Souza et al. 1996). In the southern copper belt, Pb-evaporation ages of 2733 ± 2 Ma, 2371 ± 1 Ma, and 2736 ± 4 Ma and U-Pb LA-MC-ICPMS ages for the same samples of 2729 ± 17 Ma, 2710 ± 10 Ma, and 2706 ± 5 Ma have been obtained for the high-K calc-alkaline to shoshonitic Planalto Suite (Feio et al. 2012). These ages are similar to those of the nearby IOCG deposits including Sequeirinho (U-Pb monazite age 2712 ± 5 Ma, Moreto et al. 2015b) and Pista (Re-Os molybdenite ages 2685 ± 11 Ma and 2710 ± 11 Ma, Moreto et al. 2015b).

Cu-Au (W-Sn-Bi) deposits associated with ca. 1.88 Ga granites

This group of deposits includes Breves (Tallarico et al. 2004; Botelho et al. 2005), Estrela (Lindenmayer et al. 2005; Volp

Table 1 Summary data for selected IOCG deposits in the Carajás Mineral Province

Deposit	Salobo	Igarapé Bahia	Cristalino	Sequeirinho-Pista-Baiano
Age of mineralization	2576 ± 8 Ma; 2562 ± 8 Ma (Re-Os molybdenite)	2575 ± 12 Ma (SHRIMP Pb-Pb monazite); 2537 ± 6 Ma (Ar-Ar biotite)	2700 ± 29 Ma (Pb-Pb leaching of chalcopyrite and pyrite); 2388 ± 5 Ma (Ar-Ar biotite)	2710 ± 11 Ma (Re-Os molybdenite); 2712 ± 5 Ma (LA-ICP-MS monazite)
Host rocks	Xingu gneiss and volcano-sedimentary rocks of the Salobo Group	Volcano-sedimentary rocks of the Igarapé Bahia Group	Mafic to felsic metavolcanic rocks and BIF of the Grão Pará Group	Granite, gabbronorite, and félsic metavolcanic rocks
Sodic and sodic-calcic alteration	No (minor ab with Fe-silicate alteration)	None reported	Ab and scp	Ab-hem and ab-act-mag-ap
K-Fe alteration	Kfs-bt-mag-Fe-Mg amp	Kfs-bt-mag	Kfs-bt-mag	Kfs-bio-mag
Ore mineralogy	Ccp, bn, cct with minor mol, cobaltite, safflorite, and gold	Ccp, bn with minor mol, gn, cobaltite, hessite, altaite, cst, ferberite, sch, and gold	Ccp and minor py, bravoite, cobaltite, millerite, vaesite, bn, cct, and gold	Ccp, mag, po, py and minor mol, sp., siegenite, millerite, Pd-melonite, gn, cst, hessite, and gold
U-Th	Urn	Urn, uranophane, thr, thorianite	Urn	Thorianite
F-Cl	Fl	Fl, scp, ferropyrosmalite	Fl	
REE-P	Aln, ap	Aln, parisite, bastnasite, mnz, ap	Aln, ap	Aln, ap, mnz
B-Li-Be	Tur	Tur	Tur	Tur
References	Requia and Fontboté 2000; Requia et al. 2003	Tallarico et al. 2005; Dreher et al. 2008	Huhn et al. 1999a, Ribeiro et al. 2009; Soares et al. 2001; this study	Monteiro et al. 2008a, b; Moreto et al. 2015a, b

ab albite, *act* actinolite, *aln* allanite, *amp* amphibole, *ap* apatite, *bn* bornite, *bt* biotite, *ccp* chalcopyrite, *cct* chalcocite, *cst* cassiterite, *fl* fluorite, *gn* galena, *hem* hematite, *Kfs* K-feldspar, *mag* magnetite, *mnz* monazite, *mol* molybdenite, *py* pyrite, *sch* scheelite, *scp* scapolite, *sp.* sphalerite, *thr* thorite, *tur* tourmaline, *urn* uraninite

2005), and Gameleira (Lindenmayer et al. 2001; Pimentel et al. 2003; Marschik et al. 2005) where mineralization occurs in the altered roof zones of Paleoproterozoic A-type granite cupolas and in related quartz ± carbonate-rich vein and breccia systems. Other deposits that appear to form part of this group are the vein/breccia-hosted Alvo 118 (Torresi et al. 2012), Águas Claras (da Silva and Villas 1998), and Sossego-Curral (Monteiro et al. 2008a, b; Moreto et al. 2015a) deposits. In addition to Cu-Fe sulfides, gold, and abundant quartz, these deposits commonly contain a variety of B, Be, F, Li, Sn, W, and Bi minerals (Table 2).

Sampled granite-related deposits: geology and biotite paragenesis

Alvo 118

Cu-Au mineralization at Alvo 118 (Fig. 2a) occurs within mafic-intermediate metavolcanic rocks (Grão Pará Group), gabbro, and granodiorite-tonalite (Torresi et al. 2012). Dacitic and rhyolitic porphyry dykes crosscut mineralized breccia zones at the gross scale, but locally contain magnetite and chalcopyrite, suggesting they were present during part of the alteration and mineralization (Torresi et al. 2012).

Torresi et al. (2012) recognized early alteration types including sodic alteration (albite, scapolite ± magnetite), potassic alteration (K-feldspar and/or biotite ± magnetite and quartz), and later chlorite alteration which is the most pervasive and widespread alteration. Chlorite alteration is succeeded by a second potassic alteration stage (K-feldspar, biotite, and magnetite) and later quartz and carbonate infill in breccias and veins which host the mineralization (Torresi et al. 2012). Chalcopyrite ± magnetite ± hematite and a variety of minor phases (Table 2) occur as infill within the veins and also as a separate vein stage where chalcopyrite is also abundant as an alteration of earlier chlorite.

Tallarico (2003) used SHRIMP ^{207}Pb-^{206}Pb dating of xenotime from the sulfide-rich veins to date the mineralization at 1868 ± 7 Ma (1σ, n = 12, MSWD = 1.3), with another sample from breccia-hosted mineralization at 1869 ± 7 Ma (1σ, n = 12, MSWD = 1.2).

Breves

Breves (Tallarico et al. 2004; Botelho et al. 2005; Fig. 2b) is a greisen- and vein-style Cu-Au-(W-Bi-Sn) deposit hosted within a cupola of monzogranite to alkali feldspar granite and adjacent sandstone and siltstone of the Águas Claras Formation. The granite has a range of textural types including biotite-muscovite-bearing fine-grained, granophyric, and granular hypidiomorphic types, and also has a minor episyenite zone (Tallarico et al. 2004). The massive greisen zone occurs in the

Table 2 Summary data for selected granite-related Cu-Au deposits in the Carajás Mineral Province

Deposit	Breves	Estrela	Gameleira	Alvo 118	Sossego-Curral
Age of mineralization	1872 ± 7 Ma (SHRIMP Pb-Pb monazite and xenotime); 1886 ± 5 Ma (Ar-Ar biotite)	2.7 Ga (Re-Os molybdenite); 1857 ± 98 Ma (Sm-Nd whole-rocks); 1896 ± 7 Ma (Ar-Ar biotite)	2614 ± 14 Ma (Re-Os molybdenite); 1839 ± 15 Ma (Sm-Nd whole-rocks); 1908 ± 7 Ma (Ar-Ar biotite)	1869 ± 7 Ma (massive ore) and 1868 ± 7 Ma (vein ore) (SHRIMP U-Pb xenotime); 1885 ± 4 Ma (Ar-Ar biotite)	1879 ± 4 Ma, 1904 ± 5 Ma, 1890 ± 6 Ma (LA-ICP-MS monazite)
Age of associated granite	1878 ± 8 and 1880 ± 9 Ma (SHRIMP Pb-Pb zircon)	1875 ± 2 Ma (U-Pb zircon)	1874 ± 2 Ma (U-Pb zircon – Pojuca granite), 1583 + 9/−7 Ma (Sm-Nd whole-rock)		
Host rocks	Sandstone and siltstone (Águas Claras Formation) and granite	Andesitic volcanics, gabbro, rhyolite and BIF (Grão Pará Group) and Estrelinha granite	Mafic to intermediate volcanics, amphibolite, schist and BIF (Salobo Group) and granite	Mafic and intermediate metavolcanics (Grão Pará Group), granite, gabbro and porphyry dykes	Sossego granite and gabbro
Sodic and sodic-calcic alteration	None reported	Qz-ab-mag-hst/prg	Bt-qz-ab-tur ± grt ± act	Ab-scp-mag	Weak ab-cal and ab-qz-cal-ep
Early K-Fe alteration (Archean IOCG-related?)		Bt-mag ± sulfides including mol[1]	Bt-mag-gru-sulfides including mol[1]	Kfs-bt-mag, chl	Kfs-bt-mag
Granite-hosted alteration	Kfs-bt, ms-chl, Kfs episyenite	Ab-Li-mica-tpz greisen, Kfs episyenite	Kfs episyenite?		
Paleoproterozoic veins/breccias	Qz-bt[2]-tur-chl-ms-fl-sulfides	1. Qz-ab-bt[2]-fl-mag-sulfides, 2. Qz-ms-fl-tpz	Qz-ab-bt[2]-tur-fl-cc-sulfides	Qz-cc-bt[2]-mag-sulfides → ser	1. Qz-cc-bt-chl-ep-sulfides, 2. Qz-cc-ms-hem
Ore mineralogy	Ccp, apy, lo, py, po, mol, bismuthinite, native bismuth, ferberite, sch, cst, stannite, Nb-rutile, safflorite, glaucodot, hedleyite, gold	Ccp, py, po, mol and rare cst, gold	Ccp, bn, mol and minor cobaltite, Co-pn, cst, bismuthinite, gold	Ccy, bn, py and minor sp., gn, cst, petzite, stutzite, hessite, altaite, and gold	Ccp, py, mol, siegenite, mlr, Pd-melonite, hessite, cst, gn, sp., gold
U-Th	Urn, thr	Urn	Urn	Thr, yttrialite	Urn, thorianite
F	Fl	Fl, tz	Fl	Fl	
P-REE	Mnz, xtm, ap, aln, bastnäsite	Ap	Ap, aln (synchisite, caysichite)	Ap, xtm, aln, mnz, britholite-Y	Ap, mnz
B-Li-Be	Tur, phenacite, brl, spd, micas	Tur, znw, lpd	Trm (bavenite, hellandite, gadolinite)	Gadolinite	
References	Tallarico et al. 2004; Bothelho et al. 2005; this study	Lindenmayer et al. 2005; Volp 2005; this study	Machado et al. 1991; Villas, 1999; Lindenmayer et al. 2001; Marschik et al. 2005; Pimentel et al. 2003; Grainger et al. 2008; this study	Torresi et al. 2012; Tallarico 2003, this study	Monteiro et al. 2008a, b Moreto et al. 2015b

ab albite, *act* actinolite, *aln* allanite, *amp* amphibole, *ap* apatite, *apy* arsenopyrite, *bn* bornite, *brl* beryl, *bt* biotite, *cal* calcite, *ccp* chalcopyrite, *cct* chalcocite, *chl* chlorite, *cst* cassiterite, *ep* epidote, *fl* fluorite, *gn* galena, *grt* garnet, *hem* hematite, *hst* hastingsite, *Kfs* K-feldspar, *lo* loellingite, *lpd* lepidolite, *mag* magnetite, *mlr* millerite, *mnz* monazite, *mol* molybdenite, *ms* muscovite, *pn* pentlandite, *po* pyrrhotite, *prg* pargasite, *py* pyrite, *qz* quartz, *sch* scheelite, *scp* scapolite, *sp.* sphalerite, *spd* spodumene, *thr* thorite, *tpz* topaz, *tur* tourmaline, *urn* uraninite, *xtm* xenotime, *znw* zinnwaldite

[1] Previous Re-Os dating

[2] Ar-Ar dating this study

( ) Pojuca Granite alteration

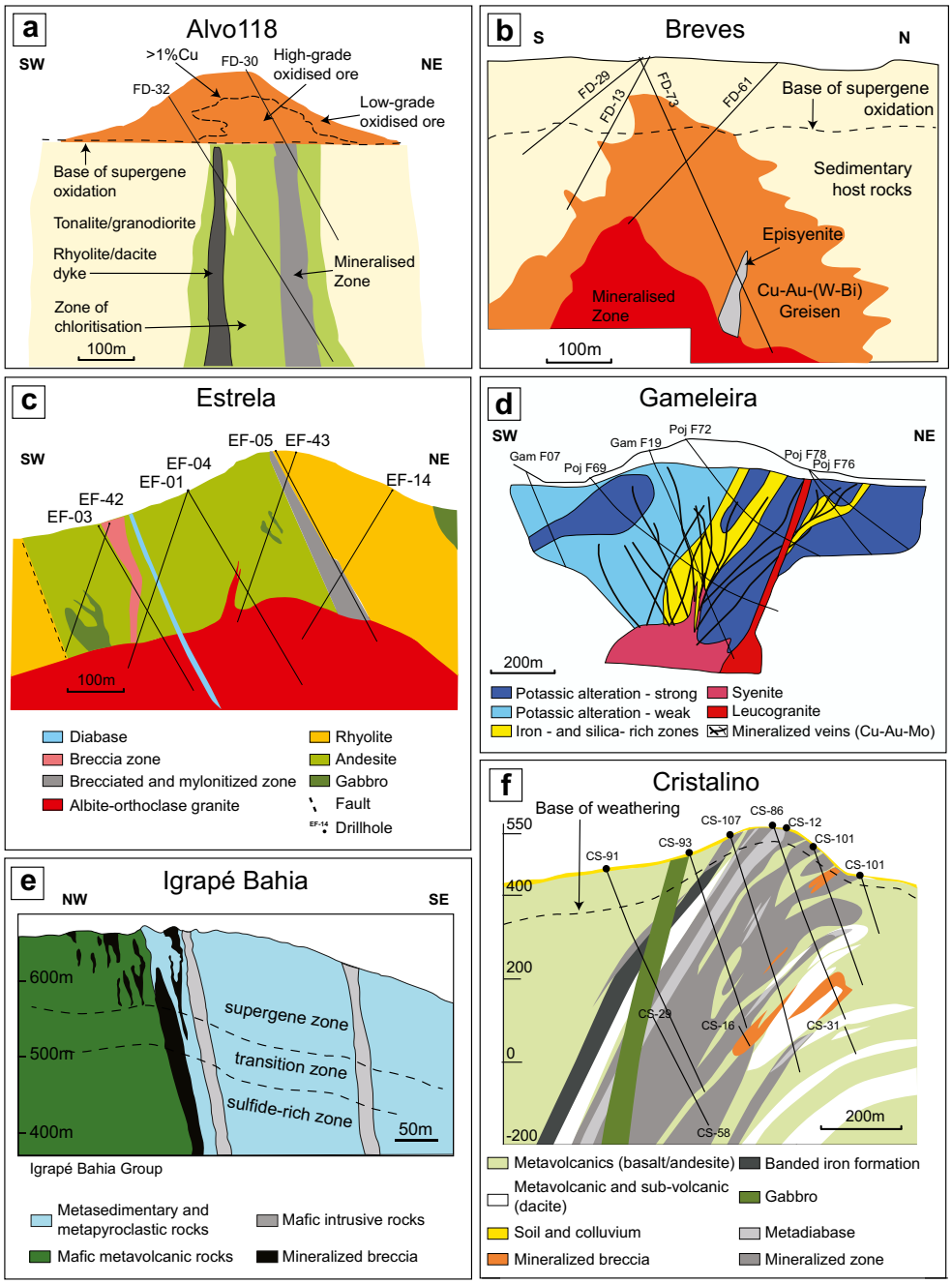

Fig. 2 Cross-sections of selected Cu-Au deposits in the Carajás Mineral province. **a** Alvo 118 (Grainger et al. 2008). **b** Breves (Tallarico et al. 2004). **c** Estrela (Lindenmayer et al. 2005). **d** Gameleira (Lindenmayer et al. 2001). **e** Igarapé Bahia (Galarza et al. 2008). **f** Cristalino (Soares et al. 2001)

upper part of the granite and extends into the host rocks with progressively decreasing alteration intensity. An early stage of potassic alteration is composed mainly of K-feldspar and biotite, together with fluorite, tourmaline, phenakite, cassiterite, and sulfides (chalcopyrite, pyrite, and pyrrhotite) (Botelho et al. 2005). The main greisen stage is composed of quartz, muscovite (commonly replaced by chlorite), fluorite, tourmaline, and chalcopyrite with a wide variety of associated minerals (Table 2). Several vein and breccia types have been recognized (Tallarico et al. 2004; Botelho et al. 2005) including (1) quartz veins that can be vuggy or filled with chalcopyrite, ferberite, and chlorite; (2) fluorite, chalcopyrite, arsenopyrite, chlorite, and quartz veins; (3) chalcopyrite-tourmaline veins; and (4) zoned veins with beryl-rich rims and centers with tourmaline, fluorite, and arsenopyrite, together with trace amounts of bismuthinite, ferberite, wolframite, monazite, galena, and spodumene.

The granite at Breves has a weighted mean SHRIMP ^{207}Pb-^{206}Pb zircon age of 1879 ± 6 Ma (1σ, n = 33, MSWD = 1.2) and mineralization has been dated by a combined SHRIMP ^{207}Pb-^{206}Pb age of 1872 ± 7 Ma (1σ, n = 14, MSWD = 1.2) for monazite and xenotime from a quartz-arsenopyrite-chalcopyrite vein (Tallarico et al. 2004).

Estrela

The Estrela Cu-Au deposit (Fig. 2c) is situated near the faulted contact between mafic-felsic metavolcanic rocks, banded iron formation, and metasedimentary rocks of the Grão Pará Group and metarhyolite (Lindenmayer et al. 2005). This sequence has been intruded by a porphyritic to equigranular alkali feldspar-topaz-Li mica granite (Lindenmayer et al. 2005). The granite contains abundant aplite, pegmatite, and stockscheider zones together with unidirectional solidification textures (UST's), miarolitic cavities (Volp 2005), and episyenite (Lindenmayer et al. 2005). Quartz-K-feldspar-biotite-chalcopyrite veins are common in the granite (Lindenmayer et al. 2005), and the upper part of the cupola consists of quartz-fluorite-mica-topaz-sulfide greisen (Volp 2005).

Lindenmayer et al. (2005) recognize early sodic-calcic alteration of the metaandesites at Estrela composed of quartz, albite, hastingsite-pargasite, magnetite, and ilmenite. This is overprinted by a potassic stage that includes biotite, albite, quartz, tourmaline, chalcopyrite, pyrite, pyrrhotite, and molybdenite (Lindenmayer et al. 2005). The main mineralization at Estrela consists of millimeter- to meter-scale quartz-rich veins, breccias, and associated alteration within the host rocks above the granite cupola. The main vein stage is composed of quartz-albite-biotite-fluorite-chalcopyrite-pyrite-pyrrhotite veins with minor magnetite, ilmenite, epidote, tourmaline, chlorite, and molybdenite (Lindenmayer et al. 2005). It is uncertain whether chlorite and epidote are later than albite and biotite. Later veins are composed mainly of quartz-white mica with minor topaz, fluorite, tourmaline, chlorite and sulfides, and late quartz-carbonate veins (Lindenmayer et al. 2005). Cassiterite, gold, and U-REE minerals are also reported (Lindenmayer et al. 2005; Volp 2005).

The granite at Estrela has been dated at 1875 ± 2 Ma and a nearby quartz-diorite at 1880 ± 5 Ma by the ID TIMS U-Pb zircon method (Lindenmayer et al. 2005). Lindenmayer et al. (2005) also report an unpublished Re-Os age for deformed molybdenite of 2.7 Ga. Volp et al. (2006) used the U-Th-Pb CHIME technique to date three monazites from aplite which gave ages of 1886 ± 19 Ma, 1827 ± 23 Ma, and 1716 ± 9 Ma. Monazite from a quartz-green biotite vein and allanite from a fluorite-sulfide vein gave ages of 1839 ± 14 Ma and ca. 1850 Ma, respectively, (Volp et al. 2006). Volp et al. (2006) noted that monazite from the quartz-green biotite vein showed evidence of alteration, but did not specify the nature of the alteration. Mineralized main stage veins (see above) have also been dated at 1857 ± 98 Ma using the Sm-Nd method on whole-rock samples of vein material (Lindenmayer et al. 2005).

Gameleira

The Gameleira Cu-Au deposit (Lindenmayer et al. 2001; Marschik et al. 2005; Fig. 2d) is essentially a vein and breccia deposit situated above a cupola of syenogranite to alkali feldspar granite which has been correlated with the nearby Pojuca Granite (U-Pb zircon age 1874 ± 2 Ma (Machado et al. 1991; Lindenmayer et al. 2001)). The host rocks at Gameleira consist mainly of mafic to intermediate metavolcanic rocks, metagabbro and banded iron formations of the Salobo-Pojuca Group (Lindenmayer et al. 2001; Pimentel et al. 2003). Lindenmayer et al. (2001) interpreted bodies of banded rocks composed largely of quartz, magnetite, and grunerite as resulting from hydrothermal alteration.

Early alteration of the metavolcanic, metasedimentary, and metagabbroic rocks at Gameleira consists mainly of widespread brown to black biotite ± scapolite alteration in mafic-intermediate rocks that is accompanied in places by garnet (garnet-biotite-scapolite schist). The banded magnetite-rich rocks are overprinted by grunerite veins and associated alteration.

Pimentel et al. (2003) reported tourmaline, titanite, ilmenite, magnetite, apatite, and uraninite in garnet-biotite-scapolite schist. Grunerite-rich zones contain green biotite, magnetite, chalcopyrite and minor bornite, pyrite, cobaltite, pentlandite, and gold with accessory stilpnomelane, apatite, uraninite, and fluorite (Lindenmayer et al. 2001). Re-Os molybdenite dating (Marschik et al. 2005) indicates an age of 2614 ± 14 Ma for grunerite-related mineralization.

The granite contains tourmaline as a common accessory mineral together with fluorite, chalcopyrite, molybdenite, and gold (Lindenmayer et al. 2001), while the Pojuca granite contains accessory topaz, tourmaline, and fluorite as well as minor pyrite, chalcopyrite, and molybdenite (Villas 1999). UST's and miarolitic cavities are also present in the granite. The quartz-rich vein system that emanates from the granite cupola post-dates the grunerite veins (Marschik et al. 2005). The quartz-rich veins contain green biotite, albite, chalcopyrite, and bornite with minor apatite, allanite, uraninite, fluorite, tourmaline, muscovite, chlorite, molybdenite, cobaltite, Co-pentlandite, carbonate, and gold (Lindenmayer et al. 2001; Pimentel et al. 2003). Minor chalcopyrite extends from the veins into the host rocks and is associated with minor alteration of earlier magnetite and grunerite.

Sampled IOCG deposits: geology and biotite paragenesis

Igarapé Bahia

The Igarapé Bahia Cu-Au deposit (Ronz et al. 2000; Tazava and Oliveira 2000; Tallarico et al. 2000, 2005; Dreher et al. 2008; Fig. 2e) is hosted within breccia bodies within steeply dipping metavolcano-sedimentary rocks of the Igarapé Bahia Group. The latter comprise chloritized metabasalt, banded iron formation, and chert in the footwall and coarse- to fine-grained metaturbidites in the hanging wall. These rocks are in faulted contact with overlying sandstone of the Águas Claras

Formation (Tallarico et al. 2000). A series of quartz diorite and diabase dykes cut the metavolcano-sedimentary rocks and Águas Claras Formation sandstone (Tallarico et al. 2000). The quartz diorites range from unaltered to highly altered, veined, and/or brecciated, whereas diabase dykes are unaltered (Grainger et al. 2008).

Heterolithic breccias contain millimeter- to meter-scale angular to rounded clasts consisting mainly of metabasalt, banded iron formation, chert, and siliciclastic metasedimentary rocks (Dreher et al. 2008). The breccia contains a rock flour matrix (e.g., Fig. 4g of Dreher et al. 2008), which is strongly overprinted by alteration/mineralization that also occurs in veins. Breccia-hosted mineralization is composed mainly of magnetite, siderite, chlorite, amphibole, tourmaline, quartz, and chalcopyrite (Dreher et al. 2008) together with a range of minor phases (Tallarico et al. 2000; Table 2). Tallarico et al. (2005) dated monazite in the ore breccia at 2575 ± 12 Ma (SHRIMP ^{207}Pb-^{206}Pb age).

Cristalino

The Cristalino deposit (Fig. 2f) is hosted by mafic and felsic metavolcano-sedimentary rocks and banded iron formations of the Grão Pará Group which have been intruded by gabbro, diorite, and granite bodies (Huhn et al. 1999b). Alteration of the host rocks includes sodic-calcic (albite, scapolite) and potassic (biotite) assemblages which occur in veins, crackle networks, and as an overprint of earlier shear fabrics. Hydrothermal intrusive breccias up to 100 m long and 30–40 m wide (Ribeiro et al. 2009) contain rounded to angular fragments of the host rocks (including albitized fragments) with a rock flour matrix that is strongly overprinted by biotite alteration. Actinolite is common in places in fault breccias, veins, crackle networks, and overprinting shear fabrics and biotite-altered intrusive breccia.

Cu-Au mineralization at Cristalino is associated with veins, crackle networks, and breccia infill comprising early carbonate-biotite-magnetite and later sulfides including mainly chalcopyrite, minor pyrite, and Ni-sulfides (Table 1). Soares et al. (2001) provided a ^{207}Pb-^{206}Pb age of 2700 ± 29 Ma (MSWD = 657) from leaching of chalcopyrite and pyrite.

Corta Goela

Corta Goela (Fig. 1) is garimpo (small mine or prospect) hosted within foliated metaigneous rocks of the Xingu Complex. Mineralization is hosted in foliated granodiorite and mafic dykes within a broad zone (100–150 m scale) of biotite alteration that extends mainly along the regional foliation and associated 10 cm scale shear zones. The regional foliation appears to form part of the Canaã Shear Zone (Fig. 1). Chalcopyrite mineralization is associated mainly with biotite-apatite-fluorite ± quartz veins and chalcopyrite-only veins. Chlorite alteration is widespread and commonly overprints the biotite alteration. No detailed studies have been undertaken on this prospect.

GT34 Cu-Au prospect

The GT34 (Fig. 1) is a Cu-Au prospect that occurs within variably foliated granitic rocks that are overprinted by scapolite veins and alteration to the west of Sossego and Alvo 118. The granitic rocks appear to be part of the Campina Verde tonalite complex and Cruzadão granite which both have Mesoarchean ages (Feio et al. 2013). Mineralization is associated with coarse-grained clinopyroxene-amphibole ± biotite bodies with crosscutting apatite veins and later pyrrhotite-pentlandite ± chalcopyrite mineralization. No detailed studies have been undertaken at this prospect.

^{40}Ar-^{39}Ar geochronology

Samples

Biotite samples were collected from drill core at eight Cu-Au deposits and prospects including Alvo 118, Breves, Cristalino, Estrela, Gameleira, Igarapé Bahia, Corta Goela, and GT34 (Fig. 2). All the analyzed samples (Fig. 3, Table 3) are interpreted to have formed synchronous with, or earlier than, the associated Cu-Au mineralization.

The biotite sample from Alvo 118 (Fig. 3a) is from a quartz-biotite-carbonate vein which forms part of the main Cu-Au mineralization stage. The biotite sample from Breves (Fig. 3b) is from a biotite-chalcopyrite vein hosted within biotite-altered Breves granite (^{207}Pb-^{206}Pb zircon age 1879 ± 6 Ma, Tallarico et al. 2004). Biotite from Estrela (Fig. 3c) is from a quartz-biotite-chalcopyrite-pyrrhotite vein. The sample from Gameleira (Fig. 3d) is from a quartz-biotite-chalcopyrite vein forming part the quartz-rich vein system that overprints grunerite alteration. The Igarapé Bahia sample (Fig. 3e) is from minor biotite veins that crosscut magnetite and precede chalcopyrite mineralization in the magnetite-rich breccia. The Cristalino sample (Fig. 3f) is from a biotite-quartz-chalcopyrite-pyrite vein.

The sample from Corta Goela (Fig. 3g) is from a biotite-quartz-chalcopyrite vein. The sample from GT34 (Fig. 3h) is from a coarse-grained clinopyroxene vein with interstitial biotite that also occurs in fractures in clinopyroxene. The biotite appears to be partly earlier than sulfide mineralization.

Analytical techniques

Laser step heating and furnace step heating experiments were carried out at the New Mexico Bureau of Mines, Socorro, New Mexico. These instruments are used interchangeably

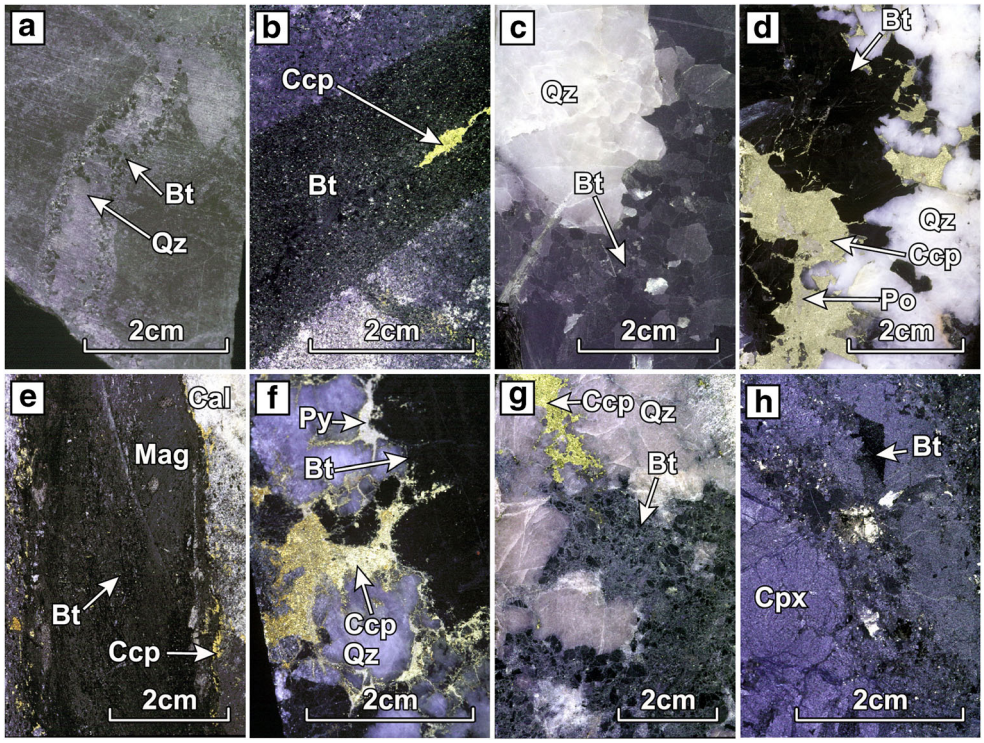

Fig. 3 Samples used for ^{40}Ar-^{39}Ar dating. **a** Alvo 118—biotite-altered mafic volcanic rock cut by a biotite-quartz vein (CJS7). **b** Breves—biotite-altered granite cut by a biotite-chalcopyrite vein (CJS20). **c** Estrela—part of a biotite-quartz-chalcopyrite vein (CJS4). **d** Gameleira—quartz-biotite-chalcopyrite-pyrrhotite vein (CJS12). **e** Igarapé Bahia—magnetite with biotite veins and later calcite-chalcopyrite. **f** Cristalino—quartz-biotite-chalcopyrite vein (CJS2). **g** Corta Goela—quartz-biotite-chalcopyrite vein (CJS16). **h** GT34—clinopyroxene vein with interstitial and vein biotite (CJS8). *bt* biotite, *cal* calcite, *ccp* chalcopyrite, *cpx* clinopyroxene, *mag* magnetite, *po* pyrrhotite, *py* pyrite, *qz* quartz

depending on scheduling and availability. Details of analytical procedures and results are given in Appendix 1, Table 3 and Fig. 4. Correction factors for interfering reactions are given in Table 3 and errors are reported at ±2σ. Data reduction and preparation of graphs and data tables used Mass Spec software (Deino 2001). The age spectra for some samples (e.g., Estrela, Gameleira, and Cristalino; Fig. 4) show increasing ages for successive steps which may indicate post-crystallization thermal disturbance. In these cases, the ages have been calculated from the higher temperature heating steps and are taken as a minimum for the age of the sample.

Inverse isochron analysis has not been used as the radiogenic yield ($^{40}Ar^*$) is generally > 99% (Appendix 1), and thus, $^{36}Ar/^{40}Ar$ will be near zero. This leads to clustered data and linear regression will provide meaningless estimates of trapped initial argon, and will not improve the estimate of preferred age.

Some samples have elevated MSWD (e.g., Igarapé Bahia and Breves) which could result from a variety of causes including post-crystallization thermal events causing partial resetting of the age spectra or minor alteration leading to ^{39}Ar recoil redistribution that can lead to some age scatter. Relatively high MSWD values are common for very old samples with high precision and likely do not invalidate the age estimate (see Schneider et al. 2007; Amato et al. 2011). Where MSWD is > 1, the age error has been increased by the square root of MSWD to provide a more conservative estimate of age uncertainty.

The K/Ca spectra (Fig. 5) have some variability which may stem from inclusions such as apatite and/or alteration by Ca-bearing phases such as calcite. Comparison of the age spectrum variation with the K/Ca spectrum variation shows no apparent correlation between the two. Mineralogical complexity indicated by K/Ca variation can lead to ^{39}Ar recoil redistribution and consequently elevated MSWD as noted above.

Results

Ages for each sample (Fig. 4, Table 3) have been calculated from the weighted mean of plateau segments except for CJS4 (Estrela) where the oldest apparent age is given (Table 3). Plateau segments are a series of consecutive heating steps yielding similar apparent ages and the number of steps and $\%^{39}Ar$ released for each sample are given in Table 3. For samples which show increasing ages for successive steps (e.g., Estrela, Gameleira, and Cristalino), this means the preferred age is calculated from only the highest temperature steps representing a small percentage (< 20%) of the released ^{39}Ar and are regarded as minimum ages. The age for the Alvo 118 sample has also been calculated from a small percentage (35.2%) of the released ^{39}Ar, but in this case, the calculated plateau age corresponds with the integrated age. The high MSWD for samples from Breves (4.54) and Igarapé Bahia (10.03) indicates statistically significant scatter about the mean.

The ^{40}Ar-^{39}Ar ages fall into two groups, an older group comprising samples from Cristalino, Igarapé Bahia, Corta Goela, and GT34 which have Paleoproterozoic to Neoarchean ages ranging from 2.2 to 2.5 Ga and a younger group comprising samples

Table 3 Summary of ^{40}Ar-^{39}Ar results and analytical methods

Sample ID	Deposit	Location	Age (Ma)	MSWD	Number of steps	%Ar39	Integrated age (Ma)	Comment
CJS2	Cristalino	FD12 483.0 m	2388 ± 5	1.3	3	18.8	2350.5 ± 3.5	Weighted mean
CJS4	Estrela	FD19 464.1 m	1896 ± 7				1880.4 ± 4.5	Oldest apparent age
CJS7	Alvo 118	FD68 246.8 m	1885 ± 4	1.92	3	35.2	1885.7 ± 2.9	Weighted mean
CJS8	GT34	GT34 255.5 m	2512 ± 7	3.26	5	75.3	2506.5 ± 4.0	Weighted mean
CJS12	Gameleira	FD57 161.1 m	1908 ± 7	3.34	7	17.5	1822.1 ± 4.1	Weighted mean
CJS16	Corta Goela	FD02 119.0 m	2193 ± 4	2.16	9	82.0	2178.1 ± 3.2	Weighted mean
CJS20	Breves	FR98 441.1 m	1886 ± 5	4.54	8	67.1	1860.6 ± 3.6	Weighted mean
CJS21	Igarapé Bahia	FD14 445.5 m	2537 ± 6	10.03	11	93.7	2520.3 ± 4.0	Weighted mean

Sample preparation and irradiation:

Mineral separates were prepared using standard crushing, heavy liquid and hand-picking techniques

The samples were loaded into a machined Al disc and irradiated. NM-140 for 100 h in L-67 position, Ford Memorial Reactor, University of Michigan and NM-145 for 52.8 h at McMaster University, Hamilton, Ontario

Neutron flux monitor Fish Canyon Tuff sanidine (FC-2). Assigned age = 28.201 Ma (Kuiper et al. 2008)

Instrumentation:

Mass Analyzer Products 215–50 mass spectrometer on line with automated all-metal extraction system

Biotite separates were step-heated with a 50 watt Synrad CO2 laser equipped with an integrator lens or Mo double-vacuum resistance furnace

Heating duration: 8 min for furnace analysis and 2 min for laser analysis

Reactive gases removed with 3 SAES GP-50 getters for furnace analysis, 2 operated at ~ 450 °C and

Reactive gases removed with 2 SAES GP-50 getters for laser analysis, 1 operated at ~ 450 °C and

1 at 20 °C. Gas also exposed to a W filament operated at ~2000 °C and a cold finger operated at − 140 °C

Analytical parameters:

Electron multiplier sensitivity averaged 9.15×10^{-17} mol/pA for laser analysis and 1.54×10^{-16} mol/pA for furnace analysis

Total system blank and background for the laser analyses averaged 273, 9.1, 1.5, 1.87, 9.9×10^{-18} mol,

and for furnace analyses averaged 793, 4.8, 0.5, 1.0, 2.4, $\times 10^{-18}$ at masses 40, 39, 38, 37, and 36, respectively

J-factors determined to a precision of ± 0.1% by CO2 laser-fusion of 4 single crystals from each of 4 or 3 radial positions around the irradiation tray

Correction factors for interfering nuclear reactions were determined using K-glass and CaF2 and are as follows:

NM-140: $(^{40}Ar/^{39}Ar)_K = 0.021 \pm 0.001$; $(^{36}Ar/^{37}Ar)_{Ca} = 0.00027 \pm 0.000015$; and $(^{39}Ar/^{37}Ar)_{Ca} = 0.0007 \pm 0.00005$

NM-145: $(^{40}Ar/^{39}Ar)_K = 0.031 \pm 0.001$; $(^{36}Ar/^{37}Ar)_{Ca} = 0.00027 \pm 0.000005$; and $(^{39}Ar/^{37}Ar)Ca = 0.0007 \pm 0.00002$

Age calculations:

Total gas age and error calculated by weighting individual steps by the fraction of ^{39}Ar released

Plateau age or preferred age calculated for the indicated steps by weighting each step by the inverse of the variance

Plateau age error calculated using the method of (Taylor, 1982)

MSWD values are calculated for n-1 degrees of freedom for plateau age

Decay constants and isotopic abundances after Min et al. (2000)

All final errors reported at ±2σ, unless otherwise noted

from Breves, Estrela, Gameleira, and Alvo 118 which have Paleoproterozoic ages between 1.88 and 1.91 Ga.

Discussion

^{40}Ar-^{39}Ar ages

^{40}Ar-^{39}Ar ages represent the time when the host mineral cooled below the blocking temperature for Ar diffusion, which in the case of biotite and muscovite ranges from approximately 300–420 °C (Harrison et al. 2009; McDougall and Harrison 1999). In several cases, this is similar to, or higher than, the temperature of mineralization interpreted from fluid inclusion and stable isotope data for the Cu-Au deposits (Lindenmayer et al. 2001; Dreher et al. 2008; Torresi et al. 2012). Comparison of ^{40}Ar-^{39}Ar dates with U-Pb and Re-Os dates requires knowledge of the ages of the primary and secondary standards used for ^{40}Ar-^{39}Ar dating accuracy, and decay constants for the decay of ^{40}K to ^{40}Ar and ^{40}Ca (Renne et al. 1988). Uncertainties in the ages of the standards and decay constants propagate into the calculated

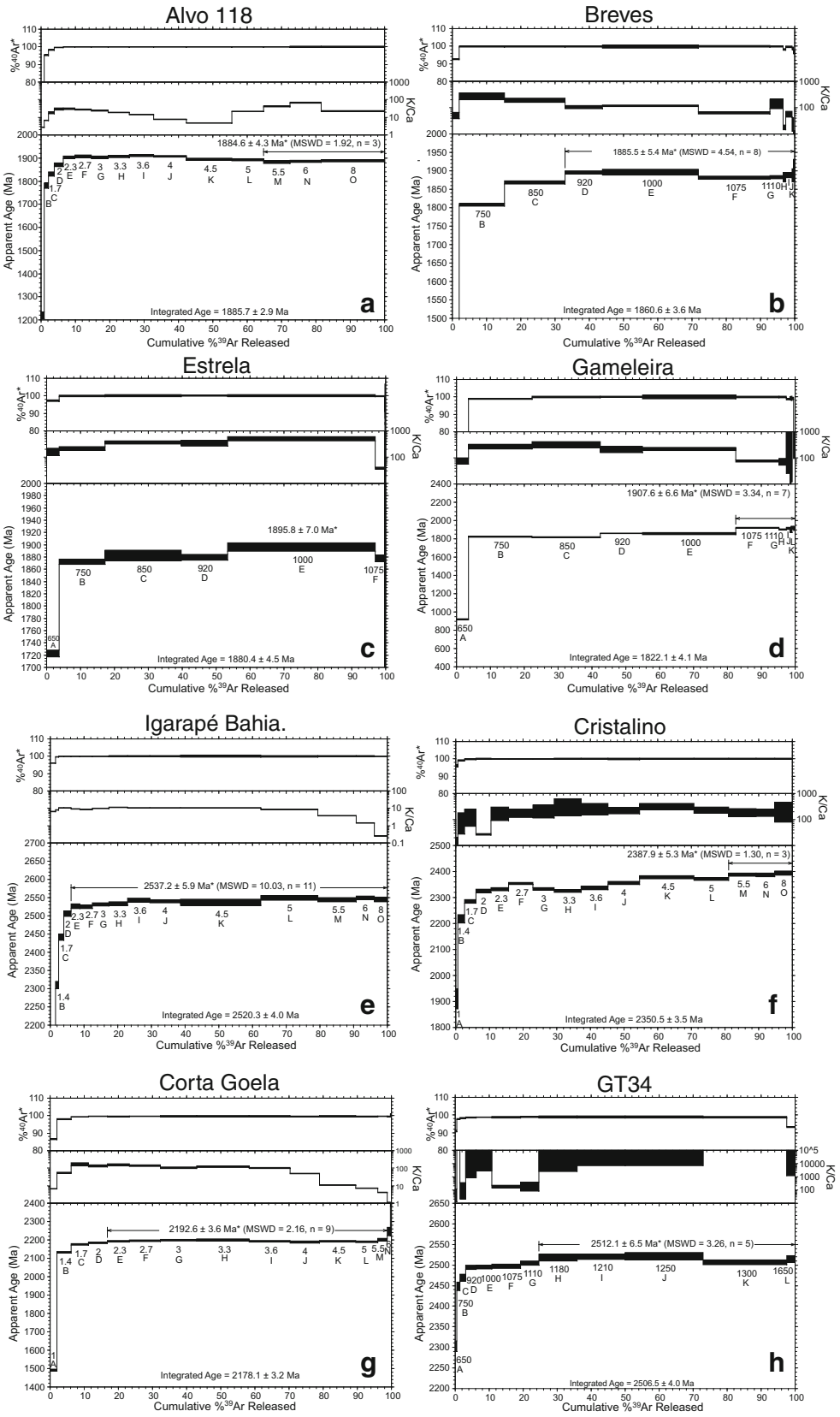

Fig. 4 ^{40}Ar-^{39}Ar age spectra for Carajás biotite samples. **a** CJS7—Alvo 118. **b** CJS20—Breves. **c** CJS4—Estrela. **d** CJS12—Gameleira. **e** CJS21—Igarapé Bahia. **f** CJS2—Cristalino. **g** CJS16—Corta Goela. **h** CJS8—GT34

age and may be > 2% (Min et al. 2000; Kuiper et al. 2008) which is larger than the analytical uncertainty.

Tallarico (2003) reported SHRIMP ^{207}Pb-^{206}Pb ages for xenotime of 1869 ± 7 Ma and 1868 ± 7 Ma for massive and

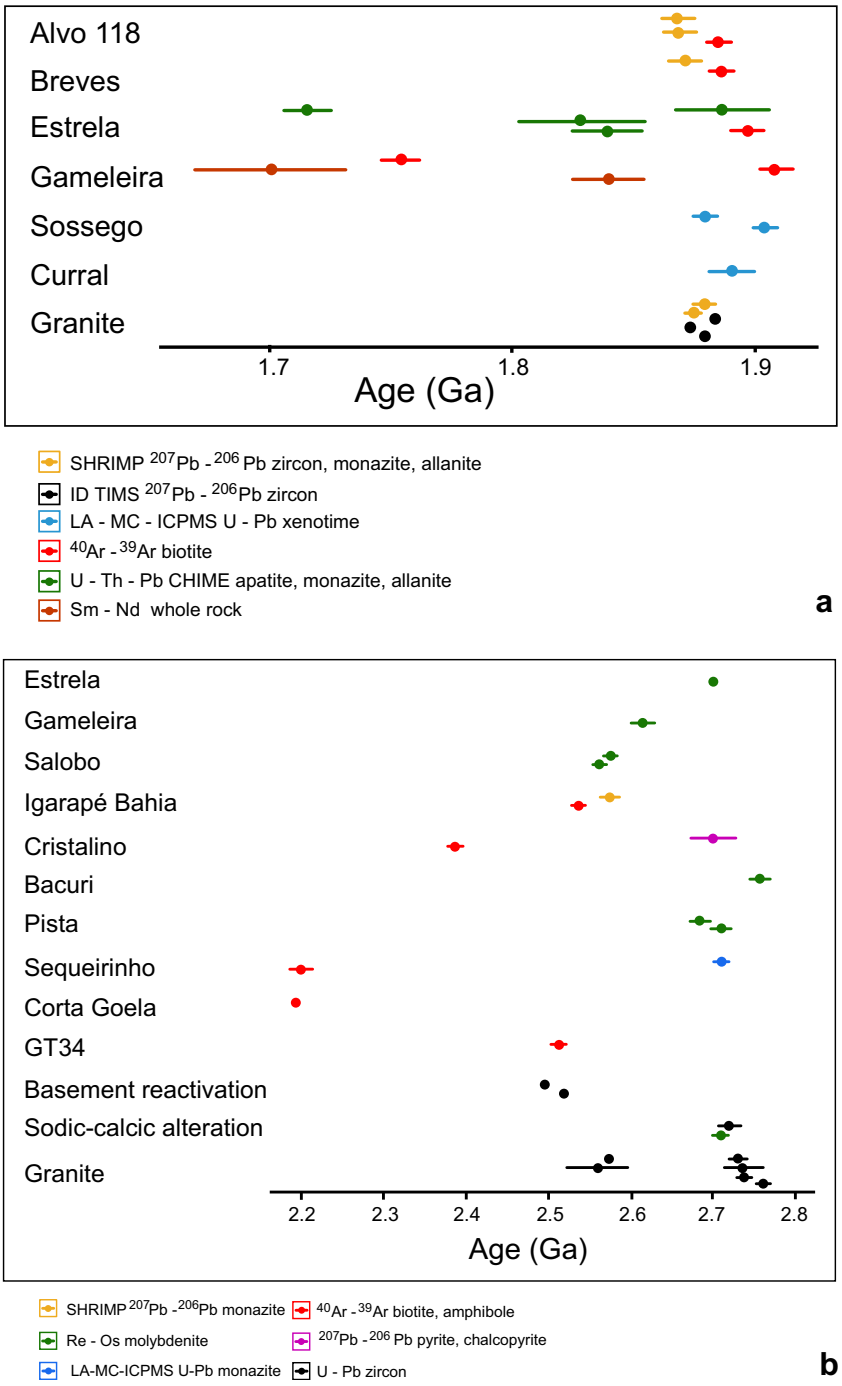

Fig. 5 Age data for granites, sodic-calcic alteration, basement reactivation and Cu-Au deposits in the Carajás Mineral Province. Error bars include only analytical uncertainty. **a** Paleoproterozoic granite and mineral deposit ages. Data from: Alvo 118—Tallarico 2003; this study; Breves—Tallarico et al. 2004; this study; Estrela—Lindenmayer et al. 2005; Volp et al. 2006; this study; Gameleira—Pimentel et al. 2003; this study; Sossego—Moreto et al. 2015; Curral—Moreto et al. 2015; Granite—Machado et al. 1991; Tallarico et al. 2004. **b** Neoarchean to Paleoproterozoic ages for granites, sodic-calcic alteration, hydrothermal minerals, and basement reactivation. Data from: Estrela—Lindenmayer et al. 2005; Gameleira—Marschik et al. 2005; Salobo—Requia et al. 2003; Igarapé Bahia—Tallarico et al. 2005; this study; Cristalino—Soares et al. 2001; this study; Moreto et al. 2015a; Moreto et al. 2015b; Sequeirinho—Moreto et al. 2015b; Marschik et al. 2003; Corta Goela—this study; GT34—this study; Basement reactivation—Machado et al. 1991; sodic-calcic alteration—Moreto et al. 2015a; this study; Granite—Avelar et al. 1999; Barros et al. 2009; Feio et al. 2012; Huhn et al. 1999a; Machado et al. 1991; Sardinha et al. 2006

vein-style mineralization, respectively, at Alvo 118. These are similar to the 1885 ± 4 Ma ^{40}Ar-^{39}Ar age reported here for biotite from vein-style mineralization (Figs. 3a, 4a, and 5a). The plateau age for this sample is the same as the integrated age (1886 ± 3 Ma; Fig. 4a) consistent with a lack of significant post-crystallization thermal disturbance.

The 1886 ± 5 Ma ^{40}Ar-^{39}Ar age reported here for biotite from a biotite-chalcopyrite vein at Breves (Figs. 3b, 4b, and 5a) is in good agreement with the 1872 ± 7 Ma SHRIMP ^{207}Pb-^{206}Pb age for monazite and xenotime from a quartz-arsenopyrite-chalcopyrite vein and 1879 ± 6 Ma SHRIMP ^{207}Pb-^{206}Pb age for zircon from the host granite (Tallarico et al. 2004). This indicates that biotite cooled through the blocking temperature for Ar diffusion within a timeframe that is likely bracketed by the analytical uncertainty.

The biotite granite which hosts quartz-mica-fluorite-topaz-tourmaline greisen-style Cu-Au mineralization a Estrela has a U-Pb zircon age of 1875 ± 2 Ma (Lindenmayer et al. 2005)

and a maximum monazite CHIME age of 1886 ± 19 Ma (Volp et al. 2006), which are similar to the 1896 ± 7 Ma ^{40}Ar-^{39}Ar age reported here for biotite from a mineralized vein (Figs. 3c, 4c, and 5a). This is consistent with vein formation being closely linked to crystallization and fluid evolution from the granite. The 2.7 Ga Re-Os age for an older, deformed molybdenite reported by Lindenmayer et al. (2005) may represent an earlier episode of mineralization linked to the early sodic-calcic and potassic (biotite) alteration. Younger monazite and allanite ages ranging from 1850 to 1716 Ma reported by Volp et al. (2006) probably reflect post-crystallization alteration which they described from one of their samples and which also appears to have affected the biotite sample used for ^{40}Ar-^{39}Ar dating in this study.

Gameleira has been the subject of several dating studies. Machado et al. (1991) presented a U-Pb zircon age (ID-TIMS) for the Pojuca Granite of 1874 ± 2 Ma and this has been correlated with the alkali feldspar granite at depth in the Gameleira deposit (Lindenmayer et al. 2001). The later leucogranite at Gameleira has a zircon U-Pb age of 1583 + 9/−7 Ma (Pimentel et al. 2003). Marschik et al. (2005) provided a Re-Os molybdenite age of 2614 ± 14 Ma for a quartz-grunerite vein from Gameleira, while Pimentel et al. (2003) gave a Sm-Nd whole-rock isochron age of 1839 ± 15 Ma for a quartz-grunerite vein. The later quartz-biotite-sulfide vein stage was also dated by the Sm-Nd whole-rock (biotite-sulfide mixtures) method at 1700 ± 31 Ma and with ^{40}Ar-^{39}Ar biotite age of 1734 ± 8 Ma (Pimentel et al. 2003). The ^{40}Ar-^{39}Ar biotite age for this vein type in the present study is 1908 ± 7 Ma (maximum age, Figs. 3d, 4d, and 5a) which is similar to the age of the Pojuca Granite. Since the quartz vein system at Gameleira is partly hosted within, and appears to be directly related to, the underlying granite, this could indicate that the alkali feldspar granite at Gameleira is similar in age to the Pojuca Granite. The 2614 ± 14 Ma Re-Os molybdenite age for a grunerite vein (Marschik et al. 2005) is considered the best age for the early alteration and mineralization since molybdenite ages are very resistant to post-crystallization disturbance (Stein 2014). The Sm-Nd ages are calculated from whole-rock samples (Pimentel et al. 2003) and may contain contributions from this older alteration and mineralization event as well as the younger vein system and therefore represent mixing between these components rather than dating individual events.

The 2537 ± 6 Ma ^{40}Ar-^{39}Ar age for breccia-hosted biotite from Igarapé Bahia (Figs. 3e, 4e, and 5b) is comparable with the 2575 ± 12 Ma SHRIMP ^{207}Pb-^{206}Pb age for monazite reported by Tallarico et al. (2005). The ^{40}Ar-^{39}Ar age spectrum has a stepwise pattern and high MSWD of 10.03 (Fig. 4e) which may reflect post-crystallization thermal disturbance and the calculated age is considered a minimum estimate for biotite crystallization. The age is indistinguishable from the SHRIMP Pb-Pb age when the uncertainties in the analyses and standards used to calibrate both techniques are considered.

The age spectrum for the Cristalino biotite has a stepwise pattern with progressively older ages for higher temperature steps (Fig. 4f). This suggests significant post-crystallization thermal disturbance and that the age calculated from the highest temperature steps (2357 ± 7 Ma, Figs. 4f and 5b) is a minimum age for biotite crystallization. This is younger than the Pb-Pb age of 2700 ± 29 Ma from leaching of chalcopyrite and pyrite (Soares et al. 2001) which is the only other estimate for the age of mineralization at Cristalino.

Biotite from the Corta Goela Cu-Au vein system has an ^{40}Ar-^{39}Ar age of 2193 ± 4 Ma (Figs. 3g, 4g, and 5b) which lies between reported ages for Cu-Au mineralization elsewhere in the Carajás region (e.g., Moreto et al. 2015a), but is similar to minimum ^{40}Ar-^{39}Ar ages (2199 ± 13 Ma) of amphibole from Sossego (Marschik et al. 2003; Fig. 5b). Additional work is required to establish the full characteristics of the mineralization at Corta Goela, but the widespread biotite and chlorite alteration and low abundances of quartz and Fe-sulfides is similar to some of the IOCG deposits in the Carajás domain. The age of biotite from Corta Goela may indicate an episode of previously unrecognized Paleoproterozoic mineralization in the Carajás district. Alternatively, the ^{40}Ar-^{39}Ar age of amphibole from Sossego (2199 ± 13 Ma, Marschik et al. 2003) is considerably younger than the U-Pb LA-ICPMS monazite age of 2712 ± 4.7 Ma (Moreto et al. 2015b) indicating a possible younger thermal event which may also have affected mineralization at Corta Goela.

Biotite from the mineralized zone at GT34 has a ^{40}Ar-^{39}Ar age of 2512 ± 7 Ma which includes all but the first few heating steps and overlaps the integrated age for the sample (Figs. 3h, 4h, and 5b). This is younger than U-Pb and Re-Os ages for the Neoarchean Cu-Au deposits but similar to U-Pb titanite ages of 2497 ± 4 Ma associated with K-feldspar alteration in the Salobo Group near the Salobo deposit and 2519 ± 5 Ma for Xingu Complex amphibolite east of Curiónopolis (Machado et al. 1991; Fig. 5b). The latter were interpreted by Machado et al. (1991) as part of a period of basement reactivation and the GT34 biotite age appears to reflect a hydrothermal event during this time. It is uncertain whether Cu-Au mineralization formed at this time or during an earlier episode of mineralization.

Despite evidence for post-crystallization thermal disturbance, the ^{40}Ar-^{39}Ar biotite dates presented here for Paleoproterozoic granite-related Cu-Au deposits in the Carajás domain are in good agreement with dating of the host granites and/or mineralization by other techniques. The ^{40}Ar-^{39}Ar biotite ages for the interpreted IOCG deposits are more problematic. The age spectra for the Igarapé Bahia and Cristalino deposits appear to have suffered from post-crystallization thermal disturbance and the ages can only be regarded as minimum estimates of the formation age. The age of the Corta Goela biotite may have been entirely reset during a post-crystallization thermal event which may also have affected the age of actinolite from Sossego. The age the GT34

biotite corresponds with that of a previously identified thermal event and it is uncertain whether Cu-Au mineralization occurred during this time or during an earlier event.

Models for ore genesis

Geochronological evidence in the Carajás Mineral Province has defined three main periods of Cu-Au mineralization at 2.72–2.68 Ga, 2.57 Ga, and 1.90–1.88 Ga (Grainger et al. 2008; Moreto et al. 2015a, b). The Neoarchean deposits are generally accepted as part of the IOCG group of Cu-Au deposits as described by Hitzman et al. (1992) and Williams et al. (2005). The main features Williams et al. (2005) considered as important characteristics of IOCG deposits include: the presence of low-Ti iron oxides, a hydrothermal origin with breccia, vein and replacement textures and specific structural control. Other common, but not essential, features include: space-time association with intrusions, association with widely metasomatized crust (Na, Na-Ca, K), and variable enrichment in F, P, Co, Ni, As, Mo, Ag, Ba, LREE and U (Williams et al. 2005). Grainger et al. (2008) described several features they considered diagnostic of the IOCG deposits in the Carajás Mineral Province including: (1) intense Fe metasomatism leading to the formation of grunerite, fayalite and/or iron oxides, (2) the extent of carbonate alteration (mainly siderite), at least in the lower temperature deposits, (3) the sulfur-poor nature of the sulfides (chalcopyrite, bornite and primary chalcocite), (4) the quartz-deficient nature of the ore systems, (5) extreme LREE enrichment (approximately $10^4 \times$ chondrite values), and (6) variable enrichment in Co, Ni, Pb, Zn, As, Bi, W, and U. In addition, several of the deposits also have widespread biotite and/or chlorite alteration of the host rocks, including Igarapé Bahia (Tallarico et al. 2005), Cristalino (Ribeiro et al. 2009), Sequeirinho (Monteiro et al. (2008a, b), Gameleira (Lindenmayer et al. 2001) and Alvo 118 (Torresi et al. 2012).

The association of Paleoproterozoic Cu-Au deposits with granites of similar age is generally acknowledged and they have been variously described as IOCG deposits (Moreto et al. (2015a, b), Cu-Au (W-Sn-Bi) deposits (Grainger et al. 2008), or as transitional deposits in the case of Alvo 118 (Grainger et al. 2008). Moreto et al. (2011) and Toressi et al. (2012) have interpreted Sossego and Alvo 118 to represent successively higher structural levels within an IOCG system where deeper alteration represented by deposits such as Sequeirinho passes upward to K-feldspar alteration at Sossego and muscovite-hematite alteration at Alvo 118.

Several of the Paleoproterozoic Cu-Au deposits (Breves, Gameleira, Estrela) have close spatial relationships with cupolas of F-, Li-, and/or B-rich granites of similar ages to the Cu-Au mineralization (Lindenmayer et al. 2001, 2005; Volp 2005; this study). The granite cupolas exhibit a variety of magmatic and hydrothermal features that are typical of crystallization and fluid saturation in volatile-rich magmas, including aplitic and pegmatitic zones, episyenite, UST's, and miarolitic cavities (Tallarico et al. 2004; Volp 2005; this study). Similar textures are a common feature of granite cupolas in Li-F-B tin-tungsten systems (Beus and Zalashkova 1964; Scherba 1970; Pollard 1983; Černý et al. 2005; Jarchovský 2006) and are consistent with a direct link between granites, massive greisens, and the overlying quartz-rich vein systems. The Carajás Paleoproterozoic granites and associated Cu-Au deposits also contain a variety of Li, F, B, P, Be, and REE phases (Table 2) that are typical of rare-element granites and pegmatites (Pollard 1995; Černý and Ercit 2005) and serve to reinforce this genetic link.

Apart from Sossego-Curral (Moreto et al. 2015a), a feature of the Paleoproterozoic Cu-Au deposits that appears to have received little attention is their common occurrence within large volumes of alteration and mineralization which form part of the Neoarchean IOCG systems. This association is best illustrated by Sossego-Curral and Alvo 118 that occur on the same regional structural system as Cristalino and Sequeirinho (Torresi et al. 2012) and is most likely due to reactivation of older structures during Paleoproterozoic transpression and extension. Paragenetic and geochronological data discussed above indicate that the ca. 1.88 Ga quartz vein systems at Gameleira and Estrela are hosted within broad zones of sodic(-calcic), K-Fe metasomatism, and possibly Cu-Au mineralization with Re-Os molybdenite ages of 2.6 and 2.7 Ga, respectively (Pimentel et al. 2003; Lindenmayer et al. 2005). The ca. 1.88 Ga Sossego-Curral deposits are hosted within an earlier alteration system associated with the 2.71 Ga Sequeirinho IOCG deposit (Moreto et al. 2015a). Alvo 118 is also hosted within an extensive system of sodic(-calcic) and K-Fe alteration including widespread chlorite alteration that is earlier than the quartz-carbonate-rich breccias and veins, and is hosted within the same regional-scale shear system that hosts Sossego and Cristalino (Torresi et al. 2012) where similar alteration is older than 2.71 Ga (Moreto et al. 2015a) and 2.39 Ga (minimum age, this study), respectively. Sodic alteration associated with the Bacaba IOCG deposit between Sossego and Cristalino has also been dated at 2.72 Ga (Moreto et al. 2015b).

The occurrence of the Paleoproterozoic Cu-Au deposits within Neoarchean IOCG-related alteration systems indicates that special care must be taken in interpreting paragenetic data for the deposits as well as models for the generation of alteration and Cu-Au mineralization in both types of systems. This is particularly important with respect to potassic alteration, especially biotite alteration, which is a feature of both types of deposits in association with Cu-Au mineralization. The Paleoproterozoic Cu-Au deposits are best considered as granite-related Cu-Au deposits that range from the granite-hosted Breves deposit, through the cupola-related Gameleira and Estrela deposits to more distal vein- and breccia-style

deposits including Alvo 118 and Sossego-Curral. The Águas Claras vein-style Cu-Au deposit (da Silva and Villas 1998) also likely forms part of this spectrum (Grainger et al. 2008), although this has had less detailed published work than the other deposits.

Are the Paleoproterozoic Cu-Au deposits of IOCG-style?

Pollard (2006) proposed an intrusion-related origin for copper-gold mineralization in IOCG deposits, including those in the Carajás Mineral Province, based on a combination of mineralogical and geochemical features of spatially and temporally related intrusive rocks, and isotopic evidence for the involvement of magmatic fluids in alteration and mineralization. The intrusive rocks typically range in composition from diorite to monzogranite and are high-K calc-alkaline to shoshonitic, magnetite-series rocks. In contrast, apart from diorite reported from Estrela, the intrusive rocks associated with the Paleoproterozoic Cu-Au deposits in the Carajás Mineral Province have a restricted compositional range from monzogranite to alkali feldspar granite, and based on the mineralogy of the granites and endogenous greisens, are variably enriched in F, Li, B, and a variety of rare elements. This is markedly different to the Lightning Creek deposit in the Cloncurry District, Australia (Perring et al. 2000), which is the only well-documented proposed source of Cu-rich fluids for the formation of IOCG mineralization. At Lightning Creek, fluids retained in granite sills from which they evolved formed albite-clinopyroxene-magnetite zones, with quartz-magnetite ± clinopyroxene ± albite veins where the Cu-rich, S-poor fluids escaped along fractures (Perring et al. 2000). The Paleoproterozoic deposits in the Carajás Mineral Province formed massive quartz, biotite, K-feldspar, (Li)-mica, fluorite, sulfide greisens where fluids were retained in the granite (Breves, Estrela), and sulfide-rich quartz ± carbonate vein systems where they escaped along fractures (Estrela, Gameleira). The Paleoproterozoic mineralization is more reduced and sulfur-rich than typical IOCG deposits.

The granites associated with the Paleoproterozoic Cu-Au deposits have much in common with A-type granites of similar, and younger, age which are widely associated with tin-tungsten mineralization in the Amazon Craton (Dall'Agnol et al. 1994, 2005; Bettencourt et al. 2005), and are generally more reduced than the magnetite-series Neoarchean granitoids. As pointed out by Grainger et al. (2008), the associated Cu-Au deposits differ significantly from the Neoproterozoic IOCG deposits in their lack of abundant Fe-oxides, S-rich Cu-Fe sulfide assemblages and their quartz-rich character. If, in addition, the components of the Neoarchean alteration systems are removed, the Paleoproterozoic deposits are essentially greisen and quartz ± carbonate-rich vein and breccia systems with little similarity to IOCG deposits. However, as with the IOCG deposits, when the fluids moved from their source, they potentially interacted with the host rocks and other fluids leading to the range of isotopic and geochemical characteristics that have been interpreted to implicate fluids from magmatic and non-magmatic sources and exchange with host rocks of different compositions (e.g., Lindenmayer et al. 2001; Chiaradia et al. 2006; Monteiro et al. 2008a, b; Dreher et al. 2008; Xavier et al. 2008, 2009, 2010; Ribeiro et al. 2009; Torresi et al. 2012). A good example is the enrichment of both Sequeirinho (~ 2.71 Ga) and Sossego-Curral (~ 1.9 Ga) in a variety of Ni sulfides and tellurides (Monteiro et al. 2008a, b; Tables 1 and 2), with Ni (Cu, Co, Pd) possibly sourced partly from meta-ultramafic rocks that occur as mylonites along nearby shear zones (Moreto et al. 2015b). However, the high Nb, Sn, W, Be, Bi, and Y contents of mineralized zones at Sossego-Curral are consistent with derivation of the ore fluids from the Paleoproterozoic granites (Monteiro et al. 2013).

The occurrence of Paleoproterozoic Cu-Au mineralization within older alteration systems raises the possibility that some components of the Paleoproterozoic systems may have been derived from the Archean IOCG systems. This possibility cannot be evaluated with present data and remains an area for future research.

Conclusions

^{40}Ar-^{39}Ar dating of biotite from Cu-Au deposits in the Carajás Mineral Province is consistent with previous geochronological work in indicating the presence of Neoarchean and Proterozoic mineralization. The ^{40}Ar-^{39}Ar data have reinforced the close temporal association between Paleoproterozoic Li-F-B granites and mineralization hosted within granite cupolas and associated vein and breccia systems (Breves, Gameleira, Estrela), and also supports previous work in viewing Alvo 118 and Sossego-Curral as more distal parts of these systems. The ^{40}Ar-^{39}Ar data suggest these deposits formed between 1908 ± 7 and 1885 ± 4 Ma. The Paleoproterozoic deposits are mostly hosted within rocks which have been affected by Neoarchean Na(-Ca) and K-Fe alteration systems, and their location is likely influenced by reactivation of the controlling structures during Paleoproterozoic transpression and extension.

In terms of genetic models, the Paleoproterozoic deposits are best seen as granite-related Cu-Au deposits and share many features in common with the styles of mineralization seen in Sn-W deposits elsewhere in the Amazon Craton. Sericitic alteration associated with Cu-Au mineralization at Sossego and Alvo 118 is considered to be part of the granite-related Cu-Au systems rather than the older IOCG systems and therefore they are not evidence for an upward transition of the IOCG-related system to sericite-hematite alteration in the Carajás Mineral province.

Acknowledgements Financial and logistical support from Vale is gratefully acknowledged. Pat Williams, Fernando Tallarico, and Matt Heizler are thanked for comments on an earlier version of the manuscript. Reviews by Lena Monteiro and an anonymous reviewer resulted in considerable improvement to the final presentation. Dalibor Bodonji kindly drafted the diagrams.

References

Amato JM, Heizler MT, Boullion AO, Sanders AE, McLemore VT, Toro J, Andronicos CL (2011) Mesoproterozoic (1.46 Ga) magmatism and exhumation during crustal extension in the Mazatzal Province: the Burro Mountains gneiss dome, southern New Mexico, Geol Soc Am Bull, doi: https://doi.org/10.1130/B30337.1, 2011

Augusto RA, Monteiro LVS, Xavier RP, Souza Filho CR (2008) Zonas de alteração hidrotermal e paragênese do minério de cobre do Alvo Bacaba, Província Mineral de Carajás (PA). Revista Brasileira de Geociências 38:263–277

Avelar VG, Lafon J-M, Correia FC, Macambira EMB (1999) O magmatismo Arqueano de região de Tucumã-Provincia Mineral de Carajás: Novos resultados gochronológicos. Revista Brasileira de Geoci ncias 29:453–460

Barros CEM, Sardinha AS, Barbosa JPO, Macambira MJB, Barbey P, Boullier A-M (2009) Structure, petrology, geochemistry and zircon U/Pb and Pb/Pb geochronology of the synkinematic Archean (2.7 Ga) A-type granites from the Carajás metallogenic province, northern Brazil. Can Mineral 47:1423–1440

Bettencourt JS, Leite WB Jr, Goraieb CL, Sparrenberger I, Bello RMS, Payolla BL (2005) Sn-polymetallic greisen-type deposits associated with late-stage rapakivi granites, Brazil: fluid inclusion and stable isotope characteristics. Lithos 80:363–386

Beus AA, Zalashkova NY (1964) Postmagmatic high temperature metasomatic processes in granitic rocks. Int Geology Rev 6:68–81

Botelho NF, Moura MA, Teixeira LM, Olivo GR, Cunha LM, Santana MU (2005) Caracteriza ão geológica e metalogenética do depósito de Cu ± (Au, W, Mo, Sn) Breves, Carajás. In: Marini OJ, Queiroz ET, Ramos BW (eds) Caracteriza ão do depósitos minerais em distritos mineiros da Amazônia. DMNP-CT-mineral/FINEP-ADIMB, pp 339–389

Černý P, Ercit TS (2005) The classification of granitic pegmatites revisited. Can Mineral 43:2005–2026

Černý P, Blevin PL, Cuney M, London D (2005) Granite-related ore deposits: geology, space-time distribution, and possible modes of origin. In: Hedenquist JW, Thompson JFH, Goldfarb RJ, Richards JP (eds) Economic geology hundredth anniversary volume, pp 337–370

Chiaradia M, Banks D, Cliff R, Marschik R, De Haller A (2006) Origin of fluids in iron oxide-copper-gold deposits: constraints from δ^{37}Cl, $^{87}Sr/^{86}Sr_i$ and Cl/Br. Mineral Deposita 41:565–573

Dardenne MA, Ferreira Filho CF, Meirelles MR (1988) The role of shoshonitic and calc-alkaline suites in the tectonic evolution of the Carajás District, Brazil. J Geophys Res 92(B9):9175–9192

Deino AL (2001) Users manual for mass spec v. 5.02. Berkeley Geochronology Center Special Publication 1a

Dall'Agnol R, Lafon J-M, Macambira MJB (1994) Proterozoic anorogenic magmatism in the central Amazonian Province: Geochronological, petrological and geochemical aspects. Mineral Petrol 50:113–138

Dall'Agnol R, Teixeira NP, Rämö OT, Moura CAV, Macambira MJB, Oliveira DC (2005) Petrogenesis of the Paleoproterozoic rapakivi A-type granites of the Archean Carajás metallogenic province, Brazil. Lithos 80:101–129

DOCEGEO (1988) Revisão litoestratigráfica da Província Mineral de Carajás – Lito estratigrafia e principais depósitos minerais. 35th Congresso Brasileiro de Geologia, Brazil, November 6-13, 1988, PRO 11–54

Dreher AM, Xavier RP, Taylor BE, Martini SL (2008) New geologic, fluid inclusion and stable isotope studies on the controversial Igarapé Bahia Cu-Au deposit, Carajás Province, Brazil. Mineral Deposita 43:161–184

Feio GRL, Dall'Agnol R, Dantas EL, Macambira MJB, Gomes ACB, Sardinha AS, Oliveira DC, Santos RD, Santos PA (2012) Geochemistry, geochronology, and origin of the Neoarchean Planalto granite suite, Carajás, Amazonian craton: A-type or hydrated charnockitic granites? Lithos 151:57–73

Feio GRL, Dall'Agnol R, Dantas EL, Macambira MJB, Santos JOS, Althoff FJ, Soares JEB (2013) Archean granitoid magmatism in the Canaã dos Carajás area: implications for crustal evolution of the Carajás province, Amazonian craton, Brazil. Precambrian Res 227:157–185

Galarza MA, Macambira MJB, Villas RN (2008) Dating and isotopic characteristics (Pb and S) of the Fe oxide-Cu-Au-U-REE Igarapé Bahia ore deposit, Carajás mineral province, Pará state, Brazil. J S Am Earth Sci 25:377–397

Grainger CJ, Groves DI, Tallarico FHB, Fletcher IR (2008) Metallogenesis of the Carajás Mineral Province, Southern Amazon Craton, Brazil: varying styles of Archean through Paleoproterozoic to Neoproterozoic base- and precious-metal mineralisation. Ore Geol Rev 33:451–489

Harrison TM, Célérier J, Aikman AB, Hermann J, Heizler MT (2009) Diffusion of ^{40}Ar in muscovite. Geochim Cosmochim Acta 73: 1039–1051

Hitzman MW, Oreskes N, Einaudi MT (1992) Geological characteristics and tectonic setting of Proterozoic iron oxide (Cu-U-Au-REE) deposits. Precambrian Res 58:241–287

Holdsworth RE, Pinheiro RVL (2000) The anatomy of shallow-crustal transpressional structures: insights from the Archean Carajás fault zone, Amazon, Brazil. J Struct Geol 22:1105–1123

Huhn SB, Macambira MJB, Dall'Agnol R (1999a) Geologia e geocronologia Pb-Pb do Granito Alcalino Planalto, Região da Serra do Rabo, Carajás-PA. In: 6th Simpósio de Geologia da Amazônia, Manaus

Huhn SRB, Souza CIJ, Albuquerque MC, Leal ED, Brustolin V (1999b) Decoberta do depéposito Cu(Au) Cristalino: geologia e mineraliza ão associada – Região da Serra do Rabo – Carajás-PA. In: SBG/Núcleo Norte, Simpósio de Geologia da Amazônia 6, Manaus, Boletim, pp 140–143

Jarchovský T (2006) The nature and genesis of greisen stocks in the Krásno, Slavkvoský les area, Czech Republic. J Czech Geological Survey 51:201–216

Kuiper KF, Deino A, Hilgen FJ, Krijgsman W, Renne PR, Wijbrans JR (2008) Synchronizing rocks clocks of Earth history. Science 320: 500–504

Lindenmayer ZG, Teixeira JBG (1999) Ore genesis at the Salobo copper deposit, Serra dos Carajás. In: Silva SG, Misi A (eds) Base metal deposits of Brazil. Belo Horizonte, MME/CPRM/DNPM, pp 33–43

Lindenmayer ZG, Pimental MM, Ronchi LH, Althoff FJ, Laux JH, Arújo JC, Fleck A, Baecker CA, Carvalho DB, Nowatzki AC (2001) Geologia do depósito de Cu-Au de Gameleira Serra dos Carajás, Pará. In: Jost H, Brod JA, Quieroz ET (eds) Caracteriza ão de Depósitos Auriferos Brasileiros. ADIMB-DNPM, Brasilia, pp 79–139

Lindenmayer ZG, Fleck A, Gomes CH, Santos ABS, Caron R, Paula FC, Laux JH, Pimental MM, Sardinha AS (2005) Caracteriza ão geologógica do Alvo Estrela (Cu-Au), Serra dos Carajás, Pará. In: Marini OJ, Queiroz ET, Ramos BW (eds) Caracteriza ão do depósitos minerais em distritos mineiros da Amazônia. DMNP-CT-mineral/FINEP-ADIMB, pp 157–225

Min K, Mundil R, Renne PR, Ludwig KR (2000) A test for systematic errors in $^{40}Ar/^{39}Ar$ geochronology through comparison with U/Pb analysis of a 1.1-Ga rhyolite. Geochim Cosmochim Acta 64:73–98

Machado N, Lindenmayer Z, Krogh TE, Lindenmayer D (1991) U-Pb geochronology of Archean magmatism and basement reactivation in the Carajás area, Amazon Shield, Brazil. Precambrian Res 49:329–354

Marschik R, Spangenberg JE, Leveille RA, de Almeida JA (2003) The Sossego iron oxide Cu-Au deposit, Carajás, Brazil. Mineral exploration and sustainable development. Millpress, Rotterdam 2003:331–4

Marschik R, Mathur R, Ruiz J, Leveille RA, Almeida A-J (2005) Late Archean Cu-Au-Mo mineralization at Gameleira and Serra Verde, Carajás Mineral Province, Brazil: constraints from Re-Os molybdenite ages. Mineral Deposita 39:983–991

McDougall I, Harrison MT (1999) Geochronology and thermochronology by the $^{40}Ar/^{39}Ar$ method, 2nd ed: New York, Oxford University Press, 269 p

Melo GHC, Monteiro LVS, Moreto CPN, Silva MAD (2014) Paragenesis and evolution of the hydrothermal Bacuri iron oxide-copper-gold deposit, Carajás Province, PA. Brazilian J Geology 44:73–90

Monteiro LVS, Xavier RP, Carvalho ER, Hitzman MW, Johnson CA, Souza Fihlo CR, Torresi I (2008a) Spatial and temporal zoning of hydrothermal alteration and mineralization in the Sossego iron oxide-copper-gold deposit, Carajás Mineral province, Brazil: paragenesis and stable isotope constraints. Mineral Deposita 43:129–159

Monteiro LVS, Xavier RP, Hitzman MW, Juliani C, Souza Filho CR, Carvalho ER (2008b) Mineral chemistry of ore and hydrothermal alteration at the Sossego iron oxide-copper-gold deposit, Carajás Mineral Province, Brazil. Ore Geol Rev 34:317–336

Monteiro LVS, Moreto CPN, Xavier RP, Melo GHC, Pestilho ALS, Silva, MAD, Juliani C, Santiago E (2013) Revealing the footprints of the Archean and Paleoproterozoic iron oxide-copper-gold systems of the Carajás province: Simpósio Brasileiro de Metalogenia III, Brazil, June 2–5, 2013, Proceedings pp 1–3

Moreto CPN, Monteiro LVS, Xavier RP, Amaral WS, Santos CJS, Juliani C, Souza Fihlo CR (2011) Mesoarchean (3.0 and 2.86 Ga) host rocks of the iron oxide-Cu-Au Bacaba deposit, Carajás Mineral province: U/Pb geochronology and metallogenic implications. Mineral Deposita 46:789–811

Moreto CPN, Monteiro LVS, Xavier RP, Creaser RA, DuFrane SA, Melo GHC, Silva MAD, Tassinari CCG, Sato K (2015a) Timing of multiple hydrothermal events in the iron oxide–copper–gold deposits of the Southern Copper Belt, Carajás Province, Brazil. Mineral Deposita 50:517–546

Moreto CPN, Monteiro LVS, Xavier RP, Creaser RA, Dufrane A, Tassinari CCG, Sato K, Kemp AIS, Amaral WS (2015b) Neoarchean and Paleoproterozoic iron oxide-copper-gold events at the Sossego Deposit, Carajás Province, Brazil: Re-Os and Pb-Pb geochronological evidence. Econ Geol 110:809–835

Olszewski WJ, Wirth KR, Gibbs AK, Gaudette HE (1989) The age, origin, and tectonics of the Grão Pará group and associated rocks, Serra dos Carajás, Brazil: Archean continental vulcanism and rifting. Precambrian Res 42:229–254

Perring CS, Pollard PJ, Dong G, Nunn AJ, Blake KB (2000) The Lightning Creek sill complex, Cloncurry District, Northwest Queensland: a source of fluids for Fe oxide Cu-Au mineralization and sodic-calcic alteration. Econ Geol 95:1067–1089

Pinheiro RVL, Holdsworth RE (1997) Reactivation of Archean strike-slip fault systems, Amazon region, Brazil. J Geol Soc 154:99–103

Pidgeon RT, Macambira MJB, Lafon JM (2000) Th-U-Pb isotopic systems and internal structures of complex zircons from an enderbite from the Pium Complex, Carajás province, Brazil: evidence for the ages of granulite facies metamorphism and the protolith of the enderbite. Chem Geol 166:159–171

Pimentel MM, Lindenmayer ZG, Laux JH, Armstrong R, Araújo JC (2003) Geochronology and Nd geochemistry of the Gameleira Cu–Au deposit, Serra dos Carajás, Brazil: 1.8–1.7 Ga hydrothermal alteration and mineralization. J S Am Earth Sci 15:803–813

Pollard PJ (1983) Magmatic and post-magmatic processes in the formation of rocks associated with rare-element deposits. Transactions of the Institution of Mining and Metallurgy section B. Appl Earth Sci 92:B1–B9

Pollard PJ (1995) Geology of rare metal deposits: an introduction and overview. Econ Geol 90:489–494

Pollard PJ (2006) An intrusion-related origin for Cu-Au mineralization in iron oxide copper gold (IOCG) provinces. Mineral Deposita 41: 179–187

Renne PR, Swisher CC, Deino AL, Karner DB, Owens TL, DePaolo DJ (1988) Intercalibration of standards, absolute ages and uncertainties in $^{40}Ar/^{39}Ar$ dating. Chem Geol 145:117–152

Requia KCM, Fontboté L (2000) The Salobo iron oxide copper–gold deposit, Carajás, northern Brazil. In: Porter TM (ed) Hydrothermal Iron oxide copper–gold and related deposits: a global perspective, Australian Mineral Foundation, Adelaide, pp 225–236

Requia K, Stein H, Fonboté L, Chiaradia M (2003) Re-Os and Pb-Pb geochronology of the Archean Salobo iron oxide copper-gold deposit, Carajás mineral province, northern Brazil. Mineral Deposita 38:727–738

Ribeiro AA, Suita MTF, Sial AN, Fallick AE, Eli F, Goulard EA (2009) Geoquimía de isótopos estáveis (C, S e O) das rochas encaixantes e do minéiro de Cu(Au) do depósito Cristalino, Província Mineral de Carajás, Pará. Geochim Bras 23:159–176

Ronzê PC, Soares ADV, Giovanni S, Barreira CF (2000) Alemão copper–gold (U–REE) deposit, Carajás, Brazil. In: Porter TM (ed) Hydrothermal Iron oxide copper–gold and related deposits: a global perspective. Australian Mineral Foundation, Adelaide, pp 191–202

Stein HJ (2014) Dating and tracing the history of ore formation. In: Holland HD, Turekian KK (eds) Treatise on geochemistry, second Edn. Elsevier, Oxford, 13, pp 87–118

Sardinha AS, Barros CEM, Krymsy R (2006) Geology, geochemistry, and U-Pb geochronology of the Archean (2.74 Ga) Serro do Rabo granite stocks, Carajás Metallogenetic Province, northern Brazil. J S Am Earth Sci 20:327–339

Schneider DA, Heizler MT, Bickford ME, Wortman GL, Condie KC, Perilli S (2007) Timing constraints of orogeny to cratonization: Thermochronology of the Paleoproterozoic Trans-Hudson orogen, Manitoba and Saskatchewan, Canada. Precambrian Res 153:65–95

Scherba GN (1970) Greisens. Int Geol Rev 12:114–150

Silva CMG, Villas RN (1998) The Águas Claras Cu-sulfide ± Au deposit, Carajás region, Pará, Brazil: geological setting, wall-rock alteration and mineralizing fluids. Revista Brasileira de Geociências 28:315–326

Silva MG, Teixeira JBG, Pimentel MM, Vasconcelos PM, Arielo A, Rocha WJSF (2005) Geologia e mineralizações de Fe-Cu-Au do Alvo GT46 (Igarapé Cinzento), Carajás. In: Marini OJ, Queiroz ET, Ramos BW (eds) Caracterização de depósitos minerais em distritos mineiros da Amazônia. DMNP-CT-mineral/FINEP-ADIMB, pp 94–151

Silva ARC, Villas RNN, Lafon J-M, Craveiro GS, Ferreira VP (2015) Stable isotope systematics and fluid inclusion studies in the Cu–Au Visconde deposit, Carajás Mineral Province, Brazil: implications for fluid source generation. Mineral Deposita 50:547–569

Soares ADV, Macambira MJB, Santos MGS, Vieira EAP, Masotti FS, Souza CIJ, Padilha JL, Magni MCV (2001) Depósito Cu (Au) Cristalino, Serra dos Carajás, PA: Idade de mineraliza ão com base em análises Pb-Pb em sulfetos (daos preliminaries). In SBG, Simpósio Geologia da Amazônia 7, Belém. Resumos Expandidos, CD-ROM

Souza SRB, Macambira MJB, Scheller T (1996) Novos dados geochronológicos para os granite deformados do Rio Itacaiúnas (Serra dos Carajás, PA): implica ões estratigráficas. In: Simpósio de Geologia da Amazônia, vol 5. Belém, Boletim de resumos expandidos, pp 380–383

Taylor JR (1982) An introduction to error analysis. University Science Books, Mill Valley, California, 270p

Tazava E, Oliveira CG (2000) The Igarapé Bahia Au–Cu–(REE–U) deposit, Carajás Mineral Province, northern Brazil. In: Porter TM (ed)

Hydrothermal Iron oxide copper–gold and related deposits: a global perspective. Australian Mineral Foundation, Adelaide, pp 203–212

Tolbert GE, Tremaine JW, Melchera GC, Gome CB (1971) The recently discovered Serra dos Carajis Iron deposits, northern Brazil. Econ Geol 66:985–994

Torresi I, Xavier RP, Bortholoto DFA, Monteiro LVS (2012) Hydrothermal alteration, fluid inclusions and stable isotope systematics of the Alvo 118 iron oxide-copper-gold deposit, Carajás Mineral Province (Brazil): implications for ore genesis. Mineral Deposita 47:299–323

Trendall AF, Basei MAF, de Laeter JR, Nelson DR (1998) SHRIMP zircon U-Pb constraints on the age of the Carajás Formation, Grão Pará Group, Amazon Craton. J S Am Earth Sci 11:265–277

Tallarico FHB (2003) O Cinturão Cupro-Aurífero de Carajás, Brasil. PhD thesis, Universidade Estadual de Campinas 229 p

Tallarico FHB, Oliveira CG, Figueiredo BR (2000) The Igarapé Bahia Cu-Au mineralization, Carajás Province. Revista Brasileira de Geociências 30:230–233

Tallarico FHB, McNaughton NJ, Groves DI, Fletcher IR, Figueiredo BR, Carvalho JB, Rego JL, Nunes AR (2004) Geological and SHRIMP II U-Pb constraints on the age and origin of the Breves Cu-Au-(W-Bi-Sn) deposit, Carajás, Brazil. Mineral Deposita 39:68–86

Tallarico FHB, Figueiredo BR, Groves DI, Kositcin N, McNaughton NJ, Fletcher IR, Rego JL (2005) Geology and SHRIMP U–Pb geochronology of the Igarapé Bahia Deposit, Carajás Copper–Gold Belt, Brazil: an Archean (2.57 Ga) example of iron–oxide Cu–Au–(U–REE) mineralization. Econ Geol 100:7–28

Vasquez LV, Rosa-Costa LR, Silva CG, Ricci PF, Barbosa JO, Klein EL, Lopes ES, Macambira EB, Chaves CL, Carvalho JM, Oliveira JG, Anjos GC, Silva HR (2008) Geologia e Recursos Minerais do Estado do Pará. In Vasquez ML, Rosa-Costa LT (eds), Texto Explicativo dos Mapas Geológico e Tectônico e de Recursos Minerais do Estado do Pará: Sistema de Informações Geográficas-SIG, Escala 1:1.000.000, Belém, CPRM, 329 p

Villas RN (1999) Granito Pojuca, Serra dos Carajás (PA): composição mineralógica, química mineral e controles químicos da alteração hidrotermal. Brazilian J Geology 29:393–404

Volp KM (2005) The Estrela copper deposit, Carajás, Brazil. Geology and implications of a Proterozoic copper stockwork. In: Mao J, Bierlein FP (eds) Mineral deposit research: meeting the global challenge. Springer, Berlin, pp 1085–1088

Volp K, Evins P, Meffre S (2006) EMPA and LA-ICPMS dating of hydrothermal REE-minerals from the Estrela copper deposit, Carajás, Brazil. Geochim Cosmochim Acta 70:A675

Williams PJ, Barton MD, Johnson DA, Fontboté L, De Haller A, Mark G, Oliver NHS, Marschik R (2005) Iron oxide copper-gold deposits: geology, space-time distribution, and possible modes of origin. In: Hedenquist JW, Thompson JFH, Goldfarb RJ, Richards JP (eds) Economic geology hundredth anniversary volume, pp 371–406

Xavier RP, Wiedenbeck M, Trumbell RB, Dreher AM, Monteiro LVS, Rhede D, Araújo CEG, Torresi I (2008) Tourmaline B-isotopes fingerprint marine evaporites as the source of high-salinity ore fluids in iron-oxide-copper-gold deposits, Carajás Mineral Province (Brazil). Geology 36:743–746

Xavier RP, Rusk B, Emsbo P, Monteiro LVS (2009) Composition and source of salinity of ore-bearing fluids in Cu-Au systems of the Carajás Mineral Province, Brazil. In: Proceedings of the 10th biennial meeting of the SGA 2009 (1), pp 272–274

Xavier RP, Monteiro LVS, Filho CRS, Torresi I, Carvalho ER, Dreher AM, Wiedenback M, Trumbull RB, Pestilho ALS, Moreto CPN (2010) The iron oxide copper-gold deposits of the Carajás Mineral Province, Brazil: an updated and critical review. In: Porter TM (ed) Hydrothermal iron oxide copper-gold and related deposits: a global perspective, v3 – advances in understanding of IOCG deposits. PGC Publishing, Adelaide, pp 285–306